Cape Peninsula University of Technology

DESIGN OF AN ENERGY-EFFICIENT RENEWABLE ENERGY WATER PURIFICATION SYSTEM WITH SMART METERING ENHANCEMENT

by

D'ANDRE VOSLOO

Dissertation submitted in partial fulfilment of the requirements for the degree

Master of Engineering in Energy

In the Faculty of Engineering and Built Environment

at the Cape Peninsula University of Technology

Supervisor: Prof. MTE Kahn
Co-supervisor: Dr. Vipin Balyan

Bellville
October 2023

DECLARATION

I, D'André Vosloo, declare that the contents of this proposal represent my own unaided work, and that the dissertation has not previously been submitted for academic examination towards any qualification. Furthermore, it represents my own opinions and not necessarily those of the Cape Peninsula University of Technology.

Signed:  **Date:** 22 October 2023

ABSTRACT

South Africa is facing regular water shortages as well as energy shortages. The country is surrounded by two oceans consisting of sufficient seawater to solve its water shortage. However, seawater desalination processes are highly energy intensive. Solving South Africa's water shortage to the detriment of the energy shortage in the country, is not a sustainable solution. South Africa is also home to an abundance of available solar energy, which places the country in a favourable position to generate energy from the available solar radiation through installing solar Photovoltaic (PV) panels. In order to minimize the amount of energy needed to treat one cubic meter of seawater, an energy efficient water purification plant was designed. The 1 ML/day Seawater Reverse Osmosis (SWRO) plant included smart metering to meter the total energy used from the water purification plant. Flow meters were installed on the plant to keep track of all the treated water and make it possible to calculate energy usage versus produced flow. The designed plant had a theoretical energy usage of 4.79 kWh/m³. Energy saving equipment such as Variable Frequency Drives (VFDs), an Energy Recovery Device (ERD) and smart Programmable Logic Controllers (PLCs) were incorporated to investigate the amount of energy that could be saved. The final average actual energy usage per unit of water was calculated to be 4.07 kWh/m³. This energy value included the complete water purification process from the inlet works until the network distribution of the product water. This value is well within the industry standard of 3 – 6.7 kWh/m³, and is therefore deemed to be efficient. The 0.72 kWh/m³ saving was further determined to be 19 139.76 kWh per month and ultimately, up to 229 677.10 kWh per year. The practicality of powering the 1 ML/day SWRO plant from solar energy was then investigated. The result indicated that 5 x 50 kW three phase inverters would be required to accommodate the total installed power for the water purification plant. This equates to 241 kW in total. To power the water purification plant during the day when the sun is available, 570 PV panels of 545 W each, were required. Ground mounted solar panels would have to be installed in rows within close proximity to the water purification plant. The surface area required was the main contributor in establishing that powering the 1 ML/day SWRO plant from solar energy, would not be practical. The 570 PV panels would need a total area of at least 1725.28 m². This surface area equates to 14 m x 125 m of open land being required, which is suitable for the installation of ground mounted panels. In addition, this area would need to be close to the water purification plant further adding to the impracticality of a solar solution. Blockchain technology in energy could be investigated to trace the origin of the energy feed to the water treatment plant. This technology could therefore be used to ensure that the energy powering the water purification plant originates from a renewable source, should it be required. In this way, the desalination plant can still be powered through renewable energy without the need for the available space within close proximity to the water purification plant.

ACKNOWLEDGEMENTS

I would like to thank my wife and family for the support during this MEng journey. I would also like to thank my supervisors for guiding me through the writing of this dissertation and lastly, I would like to thank the Cape Town based water treatment company for the water treatment plant information and actual water metering values.

TABLE OF CONTENTS

LIST OF FIGURES

LIST OF TABLES

ABBREVIATIONS

AC	Alternating Current
BWRO	Brackish Water Reverse Osmosis
CIP	Clean-In-Place
CSP	Concentrating Solar Power
DAF	Dissolved Air Flotation
DC	Direct Current
DOL	Direct Online
EC&I	Electrical Control and Instrumentation
ERD	Energy Recovery Device
ESS	Energy Storage System
GAC	Granular Activated Carbon
GMF	Granular Media Filters
HMI	Human Machine Interface
MCC	Motor Control Centre
MF	Microfiltration
MPPT	Maximum Power Point Tracker
NF	Nanofiltration
PLC	Programmable Logic Controller
PV	Photovoltaic
RO	Reverse Osmosis
SANAS	South African National Accreditation System
SANS	South African National Standards
SDI	Salt Density Index
SEC	Specific Energy Consumption
STC	Standard Test Conditions
SWRO	Saltwater Reverse Osmosis
TCF	Temperature Correction Factor
TDS	Total Dissolved Solids
TMP	Transmembrane Pressure
UF	Ultrafiltration
VAC	Volts Alternating Current
VFD	Variable Frequency Drive

Chapter 1: Introduction

1.1 Chapter Review

This chapter will serve as the introduction to the dissertation at hand. This chapter will include and elaborate on an introduction to the main topic of this dissertation, namely energy and water purification. Furthermore, this chapter will align the dissertation and elaborate on the background of the topic as well as significance of research, design and methodology as well as the research objectives.

1.2 Introduction

Water purification can be defined as a process where unwanted chemicals and materials are removed from a water source. During the 2018 drought, South Africa was planning for a possible “day zero”. As a result, a significant amount of time and resources were invested into the feasibility of water purification from sources such as ground water, brackish water and sea water to provide South Africa with an alternative water source. The assessment of these possibilities revealed that extracting water from boreholes and the sea, could prove to be a sustainable solution for the future. However, the sustainability of the energy sources required to provide these alternative solutions, is still to be investigated. Different water purification processes demand different amounts of energy usage and this is mostly linked to the type of water that is being treated and what type of chemicals and materials need to be removed from the water. To remove iron and manganese from groundwater, less energy would be required than to desalinate seawater to the same amount of clean useable water output. It is also a known fact that South Africans living in rural areas must travel far to water-points to collect water. This water is sometimes contaminated and not fit for use. The same communities are often not connected to the electricity grid and will have to rely on other energy types to go about their daily lives. An energy efficient renewable energy water purification plant has the possibility to solve these problems in the rural areas of South Africa. South Africa has still not recovered fully from the drought with some provinces still experiencing water scarcity.

South Africa is classified as one of the driest countries in the world. In addition, inefficient energy sources result in towns receiving unstable grid connections, no grid connections, or limited access to alternative energy sources that could be used to clean local water sources (Winter, 2018). For the last decade, Eskom has had power generation issues and have struggled to meet South Africa’s electricity needs. South Africa’s electricity needs are increasing every year as the population and economy is growing. The drought from 2018 opened the exploration of alternative water sources, and since then, multiple water purification plants have been installed and commissioned. Most of these plants are still reliant on Eskom as the primary energy source for power. There are different types of renewable energies

available in South Africa. This includes solar-Photovoltaic (PV) solar thermal, wind, biomass and hydroelectric. Some renewable energy sources are more efficient than others, whilst some can be more expensive to harness than others. Year round availability, accessibility and sustainability to different renewable energy sources will influence the design and preferred selection when it comes to harnessing these energies. Solar thermal, solar-PV and wind are the renewable energies of choice in South Africa when looking at the current installed renewable energy capacity in South Africa (USAID, 2021). Solar-PV makes for a great choice in South Africa, because of its geographical location. However, the solar-PV panels themselves are inefficient depending on what PV-panel technology is being utilised. Each type of PV-panel has its own set of advantages and disadvantages. The most efficient solution can be obtained by comparing different types of materials available for PV panels to the application at hand. The efficiency of the selected solar-PV panels will impact the amount of PV panels required to generate the required power. Wind energy is slightly more efficient than solar-PV with a maximum efficiency of 50% depending on location and wind speeds (Centre For Sustainable Systems, University of Michigan, 2020). Wind turbines require a large area where they will be mounted and are more expensive to manufacture and install.

Battery storage technology has improved drastically over the last few years and is becoming more feasible when looking at storing renewable energy in batteries for later use. Different battery technologies offer different efficiencies and performances that can be evaluated and applied to the problem at hand. Lead acid, lithium-ion and nickel cadmium are examples of different battery technologies for storing solar energy. Effective solar-PV energy is only available for 2500 hours per year in South Africa (Sola Group, 2013). During this time, enough power needs to be harnessed from the sun to power the system as well as storing residual power in the batteries for later use. Powering any system from a battery backup setup, requires planning and the use of the most efficient equipment to prolong battery backup time. The battery backup will be used to power the system during night time hours or on days where the radiation from the sun alone is insufficient. The use of efficient pumps and Variable Frequency Drives (VFDs) will contribute towards improving the efficiency and reducing the demand when the system is running from the battery backup.

Different pumps have different efficiencies at different speeds. The pump efficiency will increase with the increase in the rotational speed of the impeller up to a certain speed (Evans, 2012). VFDs can be used to control pump speeds to match optimal efficiency. VFDs limit start-up current compared to Direct Online (DOL) starters, thus decreasing the peak power needed for the system. This will effectively relate to smaller inverters and less batteries needed, for the same water output capacity.

Solar power inverters are used to convert Direct Current (DC) battery power and output Alternating Current (AC) power. “Inverters are available in single phase or three phase AC

output. It should therefore be determined which one would be more efficient. Similarly, not all pump sizes are available in single phase and thus it should be determined whether it will be more efficient to have two smaller single phase Volts Alternating Current (VAC) systems or a larger three phase system.

A smart metering system will be incorporated into the water purification system. The smart metering will measure the incoming water, water used for backwash, output water and the energy consumed by the system. With this information, the system can perform a water balance calculation and report on any water loss. By having the energy consumption data and the water output data, a daily energy consumption can be calculated per litre of water produced. This will be used to improve the system efficiency and to ultimately achieve the maximum water output for the lowest energy consumption. Different control regimes will result in different system efficiencies. Battery backup capacity will be determined by control methods such as running the system at full demand when the most energy is available and at a lower capacity during the night or on days when there is insufficient energy available.

1.3 Significance of Problem

By exploring alternative water sources, one can also explore alternative energy sources that can power these plants to create a total sustainable renewable solution. The findings and conclusions of this study will benefit the energy and water sector of South Africa by looking at the most efficient renewable source and technology available to power a water purification process. The smart metering will allow a municipality like the City of Cape Town to monitor the efficiency and water output of such processes and will be able to bill the water consumption reported by the smart metering system.

By making sure that the water treatment plant is optimized and operating as efficiently as possible with the least amount of required energy it will also reduce the energy load on Eskom for larger, more demanding water purification processes. The water purification process will relieve the water demand on the dams and could provide clean water to areas of South Africa that do not have access to clean water. The agricultural sector of South Africa can benefit greatly from this as most surface water found on farms needs to be treated before the water can be used for certain agricultural purposes. More farmers are opting for renewable energy as it is very expensive to install a new connection to a certain space on the farm.

This study will assist in selecting future technologies based on efficiency when opting to design and model an energy efficient water purification process with smart monitoring.

1.4 Research Questions

- How large is the difference in the theoretical energy consumption calculation and actual energy consumed for a water treatment plant?
- Can the efficiency of a water treatment plant be influenced by implementing different design techniques?
- Is it practical to power a water treatment plant from a renewable energy source?

1.5 Aim and Objectives

The primary aim of this dissertation is to design an energy efficient renewable energy water treatment plant with smart metering enhancement. This will be achieved through the following objectives:

- Select Ultrafiltration (UF) as the prefiltration method and Reverse Osmosis (RO) as the main purification method
- Review the design of the water treatment plant, develop the control philosophy, and determine the efficiency and energy consumption
- Gather energy data from the water treatment plant over two months
- Compare the energy consumption between actual, theoretical, and modern industry recorded values obtained from the smart metering
- Investigate the practicality of powering such a plant from a renewable energy source

1.6 Research Design and Methodology

The research design will look at recent research articles, journals and past theses that have been published in the last five (5) years. The content of these papers will relate to energy efficiency, renewable energy, water treatment plants and smart metering. The literature review will investigate each of these topics as individual topics as well as the cases where they have been combined. The literature review will evaluate the design methodologies, energy efficiency techniques and smart monitoring implementation from the oldest papers to the latest published papers. It will also investigate an efficient way of providing power to the water purification plant as well as implementing more energy efficient control and smart metering to water purification plants.

An energy efficient water purification plant with smart metering will be designed and reviewed with researched efficiency techniques for an industry customer where the actual plant will run on site where data will be gathered. The designed and calculated energy consumption will be compared with the actual energy, collected with smart metering, consumed and water produced over a period of three months. This data will ultimately be compared with previous research for a typical plant. This will form the basis of designing an energy efficient water

purification plant with smart monitoring. The actual energy consumption will then be used to look at powering such a plant with renewable energy and the practicality thereof.

No data will be gathered from humans or animals.

1.7 Significance of Research

An energy efficient renewable energy water treatment plant with smart metering enhancement will be deemed suitable for areas across South Africa where there is no access to water and there is none or limited access to electricity. The incorporated smart metering functionality will allow better control and autonomy to the design. The design and implementation of such an energy efficient water treatment plant will ensure the following benefits:

- Providing future designs with energy efficiency and enhanced control methodologies
- Can be implemented where Eskom electricity is not available or sufficient
- Providing poor communities in South Africa with clean drinking water
- Providing the local municipalities control over water treatment plant power usage and water output
- Will prevent misuse and stealing of water, through smart monitoring and metering
- Will create local jobs and benefits, with regards to daily checks and minor maintenance

1.8 Expected Outcomes of Research

The outcomes of this dissertation are expected to benefit and equip electrical design technologists/engineers as well as process design technologists/engineers with future designs to consider with emphasis on implementing more energy efficient processes that will save energy and maximize output. By the end of this dissertation, the following outcomes will have been achieved:

- Reviewing available literature with regards to RO and UF design, solar and wind renewable energies, smart monitoring and metering as well as control strategies and energy efficiency principles
- Gather all knowledge related to energy efficiency and design rules with regards to the above topics to the standard of an energy manager
- Design an energy efficient water treatment plant with smart metering capability and evaluate energy efficiency
- Formulate examples of where energy efficiency and saving techniques can be applied to a water treatment plant
- Apply researched and developed energy efficient techniques and strategies to a water treatment plant

1.9 Contributions of Research

Water treatment plants are often implemented by government where capital is limited. Maximum water production is needed for as little capital outlay as possible. This research will contribute towards future designs and energy efficiency practices towards water treatment designs. With proven energy efficiency and the possible savings, water treatment systems can be implemented and designed with energy efficiency techniques that will maximize the water output for minimal energy and capital input. This will also provide design technologists/engineers the right mindset and energy efficient methodologies to apply to their designs. This research could possibly lead to further research in future with regards to further improving efficiency or applying these principles to other renewable energy and water purification types.

1.10 Dissertation Organisation

The rest of the dissertation is organised as follows. Chapter 2 presents the water purification and energy literature review that is applicable to this dissertation. Chapter 3 presents the methodology used to obtain the results for the purification plant design as well as the energy consumption calculation. Chapter 4 presents the results and discussion section which includes the equipment selection, theoretical and actual power consumptions comparison, automation techniques applied as well as the investigation of solar power feasibility. Chapter 5 concludes all of the aforementioned chapters into the concluded findings.

Chapter 2: Water purification and energy literature review

2.1 Introduction

The 2018 drought in South-Africa served as an eye opener when it comes to water availability. Water is a resource of which limited useable quantity is available at any given stage. This opened the floor to obtaining potable water from a range of different sources including underground aquifers, surface waters and the ocean. The ocean, however, is saline and cannot be used directly as potable water without the use of a water treatment process. The same goes for water contained in underground aquifers. This water can be accessed by drilling a borehole and abstracting the water, however the quality may not be fit for human consumption. This may be as a result of certain elements within the water, or exceeded concentration limits of various elements in the water (Boadi, et al., 2020). Various methods of water treatment have been evaluated and thus classifying one water treatment process as being more efficient than another process cannot be clearly stated. Not all water purification types are suitable for treating all feed water types and many of the purification plants make use of more than one technology, usually starting with pre-filtration to eventually better the efficiency of the membrane technology down the treatment line. Without pre-treatment, membrane technologies like RO and UF efficiencies are very poor (Popescu, et al., 2017).

South Africa's electricity provider has struggled to provide enough electricity to the people of South Africa. Rolling loadshedding across the country has been crippling to the economy and has left the citizens in the dark. In conjunction with loadshedding, the price of electricity has increased by 177% in the last ten years. To add to this, the price of water has increased with 213% in the last 10 years (de Wet, 2020). As a result, many people and businesses have turned to renewable energy sources for their supply of electricity. The international costs of generating power from renewable energy sources such as solar-PV, Concentrating Solar Power (CSP), onshore and offshore wind has dropped by 82%, 47%, 39% and 29% respectively from 2010 to 2019 (IRENA, 2020). By generating electricity from renewable energies, it is possible to store this surplus energy into a form of storage. A common storage method for storing energy is in the form of a battery. Batteries are available in different types, shapes, and sizes. Conventional battery types can include lead acid and lithium-ion whilst other forms of storge can include molten salt, hydrogen, and compressed air. These forms of batteries have different power ratings, cycles, and efficiencies (Zablocki, 2019).

Smart metering is not a new concept and is used all over the world to save electricity and report on energy usage. Smart metering is also not limited to electricity but can also be seen in light of other metering instruments such as flow meters and analytical instruments used in the water and wastewater field. Current methods of collecting data includes the manual read and recording of this data (Muller & Booysen, 2014). By digitalizing this data and having it

available in real time can contribute to a more efficient control of the system and or mitigation of potential losses.

2.2 Water Purification

In the last ten (10) years, there have been many studies into powering water treatment plants with a renewable energy source since electricity access and access to clean water have both been a growing concern. It is therefore possible to solve two problems with one solution. A recent study in South Africa includes a review of different renewable energies for powering a RO system. The study indicated the possible renewable energies and the optimisation of a RO system as a general overview of available technologies. Different desalination technologies such as humidification-dehumidification method, multi-stage flash desalination method, vapour compressor distillation method of desalination, multi-effect distillation, electro-dialysis, capacitive deionisation method, membrane distillation and RO method have been discussed and reviewed (Okampo & Nwulu, 2021). Water purification that includes membrane processes can include, microfiltration, ultrafiltration, nanofiltration and RO. (Pangarkar, et al., 2011).

The different membrane processes all work on the same principle where the water is pumped over a membrane. Different membranes have pores of different sizes and will subsequently remove different pollutants. The smaller the pores, the higher the pressure needed to force the water through the pores. This will be classified as the high-pressure side, whereas the water that passes through the membrane will be classified as the low-pressure side. Table 2.1 indicates the membrane process and the particle size removed. Some of the membrane processes can overlap into the desalination process. The membranes that can overlap into the desalination process will be classified as RO and to some extent, Nanofiltration (NF) can also remove salt. The membrane process that can remove salt will also require a high-pressure pump that will assist the feed pump in increasing the pressure required for the membranes.

Table 2.1 : Membrane processes and their technical details (Pangarkar, et al., 2011)

Membrane Process	Applied Pressure (Bar)	Minimum size of particle that can be removed	Removal efficiency of pollutants (%)
Microfiltration	0.3-5	0.1-3 µm	Turbidity (>99%), Bacteria (>99.99%)
Ultrafiltration (UF)	0.3-5	0.01-0.1 µm	Turbidity (>99%), Bacteria (>99.99%), TOC (20%)
Nanofiltration (NF)	5-10	200 - 400 daltons	Turbidity (>99%), Color (>0.98%), TOC (>95%), Hardness (>90%), Sulfate (>97%), Virus (>95%)
Reverse Osmosis (RO)	10-50	50 – 200 daltons	Salinity (>99%), Color and DOC (>97%), Nitrate (85-95%), pesticide (0-100%), As, Cd, Cr, Pb, F removal (40-98%)

From Table 2.1 above it can be seen that RO can remove the smallest particles when compared to the other membrane processes, but at the expense of a higher operating pressure. To obtain the higher operating pressure, a larger pump will be required. The larger pump will require more energy.

2.3 Desalination Methods

2.3.1 Overview

A RO system with brackish feed water is referred to as a Brackish Water Reverse Osmosis system (BWRO), whereas a system with a seawater intake is referred to as a Seawater Reverse Osmosis (SWRO) system. Desalination is the process by which saline water (brackish or seawater) can be purified to potable standard by making use of a variety of technologies as seen in Fig 2.1.

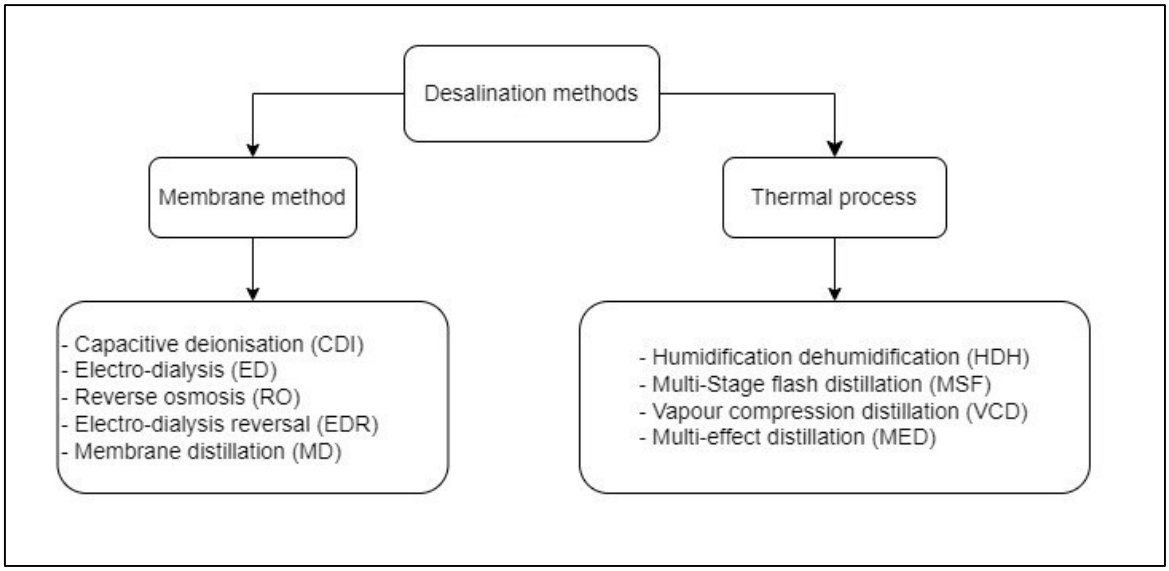

Figure 2.1: Desalination methods (Okampo and Nwulu, 2021)

Desalination through the SWRO process with seawater as the intake water source is the most energy intensive RO process. This energy consumption has dropped drastically over the last forty years due to membrane technologies, multistage configurations, Energy Recovery Devices (ERDs) etc. The Specific Energy Consumption (SEC) of modern SWRO desalination plants can range from anything between 3 – 6.7 kWh per cubic meter of product water produced (Ghaffour et al., 2015). For the purpose of this water treatment design thesis, emphasis will be placed on the membrane method, especially the RO process to drive the desalination process.

2.3.2. Reverse Osmosis

The term osmosis can be described as the principle by where water wants to move from a lower concentration to a higher concentration through a semipermeable membrane until the two solutions on either side of the membrane have reached equilibrium in concentration. This

process does not require a lot of pressure and can happen naturally at atmospheric pressure. The term RO is exactly what the name states, the osmosis process but in a reverse state. This means that water from a higher concentration flows through a semipermeable membrane to lower concentration on the other side of the membrane. The reversal of this osmosis process requires external pressure to force the water through the membrane. Fig 2.2 is a visual representation of this process in the forward and reverse state (Pangarkar et al., 2011).

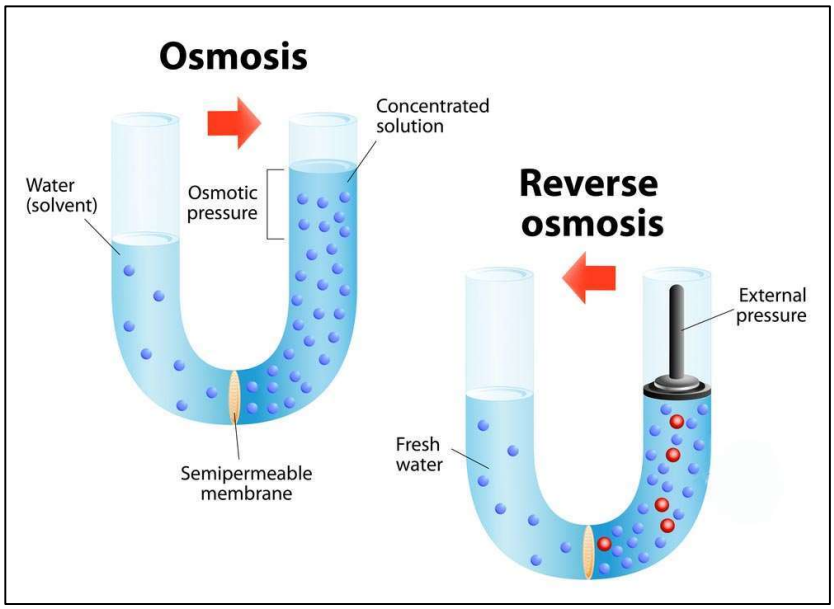

Figure 2.2: Osmosis and RO process (Water-Rightgroup, 2003)

Two of the most general types of RO systems can be classified as a BWRO or a SWRO. When treating brackish water, the Total Dissolved Solids (TDS) in the water is not as high as that of seawater, and as a result, a smaller sized high-pressure pump will be able to achieve the same amount of product flow as to when compared to seawater, where a much larger high-pressure pump will be needed to achieve the same amount of product water. TDS concentration is a good indication of the saline levels in water. The average TDS concentration of saltwater is around 35 000 mg/L whereas brackish water has a TDS concentration around 3000 to 10 000 mg/L. The upper TDS range of fresh water is estimated to be 1000 mg/L (Qiu and Davies, 2012).

RO can be subdivided into four (4) different divisions that make up the RO water treatment process. These four divisions are pre-treatment, high pressure pump, membranes and post treatment such as dosing of chemicals. Fig 2.3 below is a representation of a RO system which indicates the four (4) subdivisions of such a process.

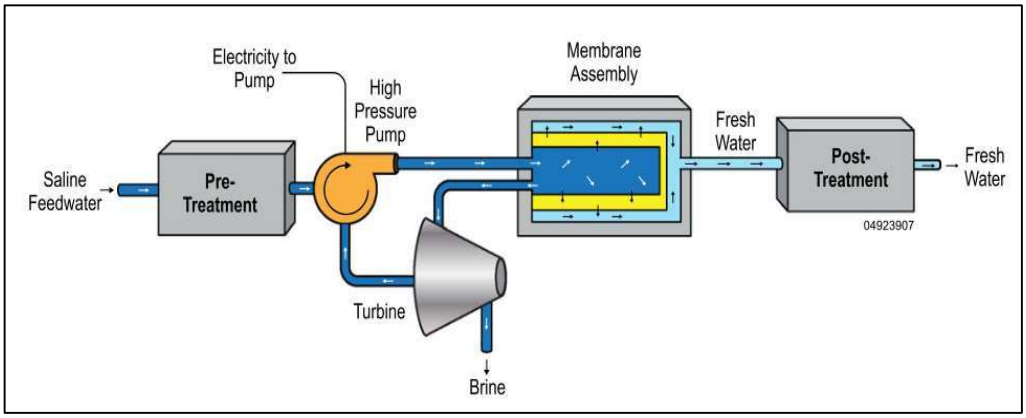

Figure 2.3: RO system (Al-Karaghouli and Kazmerski, 2013)

As seen from Fig 2.3, there is a stream called brine that is rejected from the system. Brine is a saline solution of water that is saturated with dissolved salt to the point that it cannot pass through the RO membranes. This brine rejection amount will be different for that of a BWRO and for that of a SWRO because of the different TDS concentrations.

The efficiency of such a RO system can be calculated by what is called the recovery percentage and is often used to gauge the health and operation of a RO process. The recovery percentage is a calculation that indicates how much of the total infeed water is recovered as product. A BWRO has the capability of recovering between 70 – 97 % of the feed water as product, whereas a SWRO, depending on the TDS, is limited to the 35 – 45 % range (LENNTECH, 2020).

A BWRO can have more than one membrane filtration stage. This is called a multi-stage configuration. A second stage can be designed to increase the efficiency of the process. The second stage will attempt to treat the brine rejected from the first stage to slightly increase the product output of the plant. Some systems can have as many as three stages (Qiu and Davies, 2012). The multistage efficiency increase technique is possible but not often seen on SWRO as the salinity of the brine is of such a TDS concentration that a very large high pressure pump is needed with special membranes to increase the product capacity by very little, making the capital investment for the extra product return unattractive (Ghaffour et al., 2015).

ERDs have been invented to recover some of the lost energy in the RO process. Some of the earlier methods included the Pelton Wheel and the Francis Turbine. The ERD harvests the additional energy locked up in the pressurized brine stream to then power a device that could lessen the workload of the high-pressure pump (Guirguis, 2011). Since the year 2000, the ERD's have moved from the previous mentioned centrifugal devices to isobaric chamber ERD's. The efficiency of the isobaric chamber ERD's are around 95 – 97 % because of the direct energy conversion between the pressurised brine and feed streams. With the isobaric ERD, the two streams, brine and feed, do not mix during this energy conversion process and comes directly into contact with each other. The efficiency of the previously mentioned ERD's is 85 % and 75 % respectively for the Pelton wheel and the Francis Turbine (Schunke et al.,

2020). By using the ERD's, the energy savings expected can be between 25 % and 40 % when compared to the conventional SWRO (Peñate and García-Rodríguez Lourdes, 2011). Fig 2.4 indicates a desalination SWRO with an ERD installed. It can be seen that the ERD feeds into a smaller booster pump that re-joins the feed stream to the RO membranes. This allows the design to cater for a smaller sized RO feed pump.

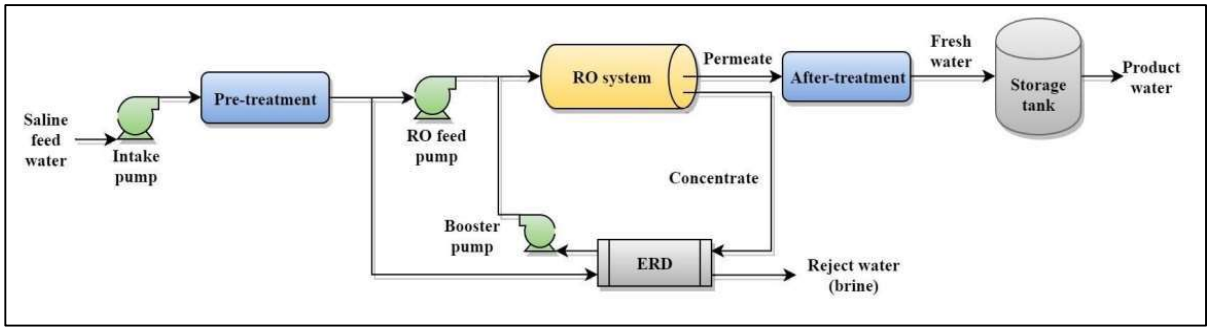

Figure 2.4: Typical SWRO design with ERD (Mito et al., 2019)

2.3.2.1. Pre-Treatment

Pre-treatment is the process where the water, in this case seawater, will be undergoing a pre-treatment process before it enters the RO membranes. This process will ensure that the feedwater to the RO membranes will be of a good consistent quality to ensure effectiveness of the RO process over the membranes. The pre-treatment process is an important step of the water purification process as this will remove solids and unwanted particles, organic matter, hydrocarbons and precipitated metals from the water that can unnecessarily foul the RO membranes. This step will increase the longevity of the RO membranes, increase the product flow and ultimately increase the efficiency of the desalination system (Bonnelye et al., 2004).

Pre-treatment for a desalination process can be carried out in several ways. This is mostly dependant on the direct intake water quality from the source. Silt, oil, solids in the water, and algae are some of the common parameters to be considered when selecting a pre-treatment process. For the purpose of this dissertation, Granular Media Filters (GMFs) and UFs will be investigated as they are the most common pre-treatment options for current desalination processes, with GMF being the most common. UF technology is gaining traction in the market because of its footprint, water quality and wide adaptability to various parameters in the intake water (Brover et al., 2022). There are many other pre-treatment methods such as Dissolved Air Flotation (DAF), Microfiltration (MF) etc. Both of these processes will achieve similar outputs, but require different equipment, which will have different energy consumptions and different efficiencies. GMF will primarily consist of filters in series or parallel, depending on the design and output requirement, that will be filled with conventional granular media which can include silica sand, Granular Activated Carbon (GAC) etc. (Engelhardt, 2012). Both the UF and GMF will consist of a feed pump and a backwash pump for each process. The energy

requirements for each process will be investigated further in a later chapter. Fig 2.5 illustrates different pre-treatment configurations for a desalination process.

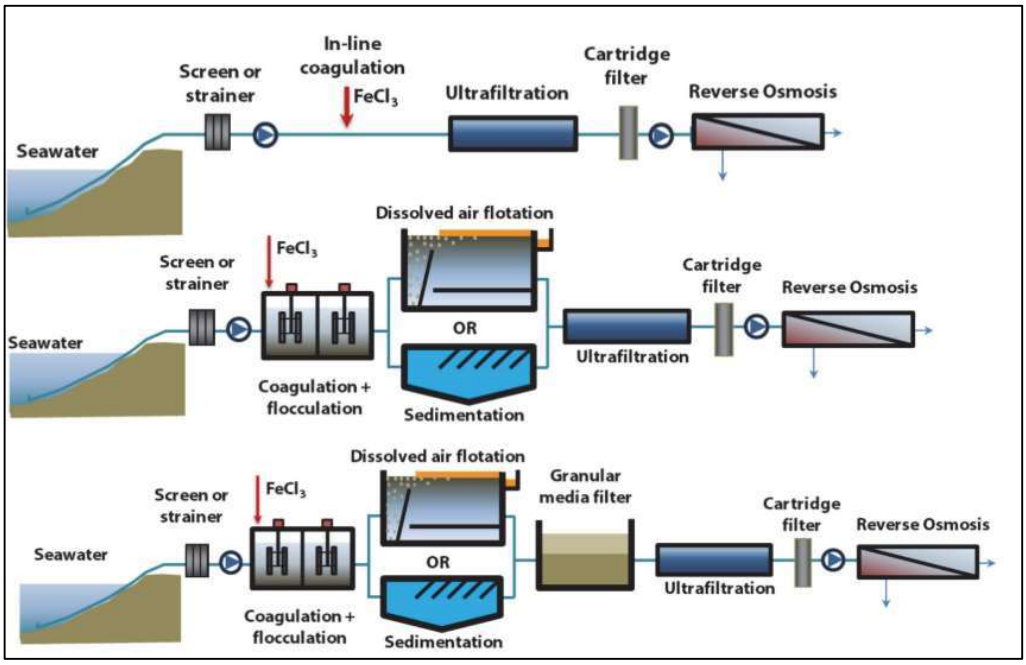

Figure 2.5: Different pre-treatment options for desalination (Tabatabai, 2014)

2.3.2.2. High-Pressure Pump

The externally required pressure to facilitate the RO process will be provided by a high-pressure pump. The high-pressure pump will perform the work needed so that the externally applied pressure is equal to the design pressure with the resultant lower concentration water gathering on the opposite side of the permeable membrane. The high-pressure pump is the piece of equipment that consumes the most energy in the RO process, typically around 50 – 75 % of the total amount of energy consumed (Gude, 2011).

2.3.2.3. Membranes

Membranes are one of the most important components of the RO process. The membranes are responsible for separating the fresh product water from the saline brine rejection, with the help of the high-pressure pump. The selection of these membranes in the design phase of the RO is important as the operating pressure of the RO, which is different for desalination, brackish water etc., will play a vital role when making the membrane selection.

The volume and type of water to be treated will influence the membrane selection. Fig 2.6 demonstrates the inner structure of a common RO cartridge membrane (Maynard and Whapham, 2019).

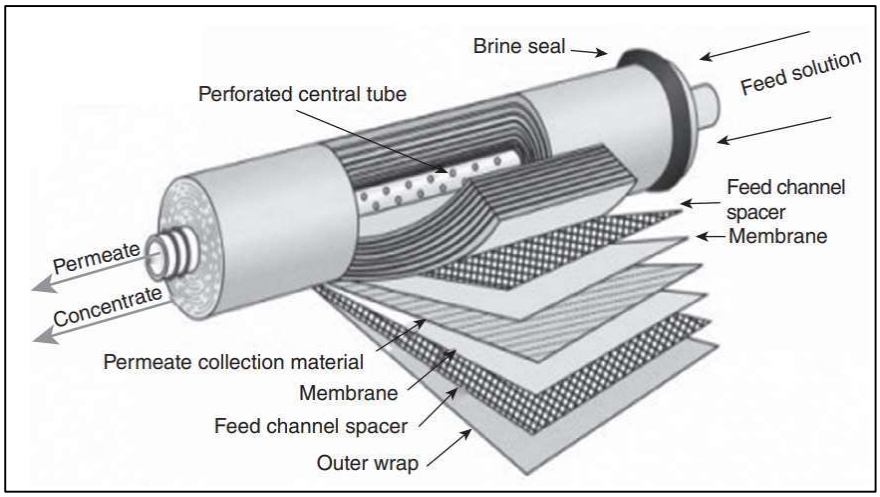

Figure 2.6: RO membrane construction (Maynard and Whapham, 2019).

Feed water will enter on one side of the membrane and the high-pressure pump will force water through the membrane. By forcing the water through the membrane material (high-pressure side), the water solution is separated into product water and saline water, subsequently removing the impurities from the product water. The product water enters the middle tube as seen in Fig 2.6. This is also referred to as the low-pressure side of the membrane. The concentrate that remains will exit the membrane on the opposite side of the feed side. The concentration can then be used as the feed solution to a second stage of RO membranes. The same process occurs, but with less product water since the feed water of the second stage is of a more saline concentration since it is the rejection water of the first stage.

A common by-product of the RO process is the fouling of the membranes during operation. (Kang and Cao, 2012). Therefore, chemical dosing is an important function that can be associated with the pre- and post-treatment of the water during the RO process. As described in the pre-treatment section of this document, the unwanted matter can seep through and reach the membranes which will then start to build a layer on the surface of the membranes, this can be removed by chemical treatment. The fouling of the membranes will decrease membrane performance and increase the amount of energy needed to produce the same unit of water.

2.3.2.4. Post-Treatment

Post-treatment of the RO water will allow the product water to reach the desired quality. The post-treatment process can vary depending on the raw product water quality. The product water can be treated for a variety of factors which can include adjusting the pH, disinfecting the water and controlling the corrosion capability of the product water (Duranceau et al., 2012). Dosing pumps can be used to dose certain amounts of chemicals to achieve the above mentioned results.

2.3.2.5. Energy Efficiency of RO Through Membrane Technology

The SEC is the most important calculated parameter that needs to be considered when designing a RO system. This is the performance indicator that will define the amount of energy needed in kilowatt-hour (kWh) for every cubic meter (m^3) of water produced. This will however be different for seawater and brackish water and cannot be directly compared to each other. The general expression for SEC for a typical membrane process can be calculated as follows from (Karabelas et al., 2018):

$$SEC = \frac{W_{TOTAL}}{Q_P} \tag{2.1}$$

$$SEC = \frac{1}{R}\left[\frac{P_f - P_0}{\eta}\right] + (1-\beta)\left[\frac{1-R}{R}\right]\left[\frac{P_0 + \eta_E \Delta P - \eta_E P_f}{\eta}\right] \tag{2.2}$$

where R = Product recovery friction

η = Efficiency of pumps

P_f = Feed pressure

P_0 = Product pressure

β = Leakage ratio of ERD

η_E = Pressure transfer efficiency of ERD

ΔP = Pressure difference across pressure vessel

The ideal SEC can be calculated by neglecting the losses in pumps and pressure equipment.

$$SEC_i = \left[\frac{1-R}{R}\right](\Delta P) + \left(P_f - P_0\right) \tag{2.3}$$

Fig 2.7 is a representation of the itemized SEC contributions to each section of the RO process. More information can be found in (Karabelas et al., 2018).

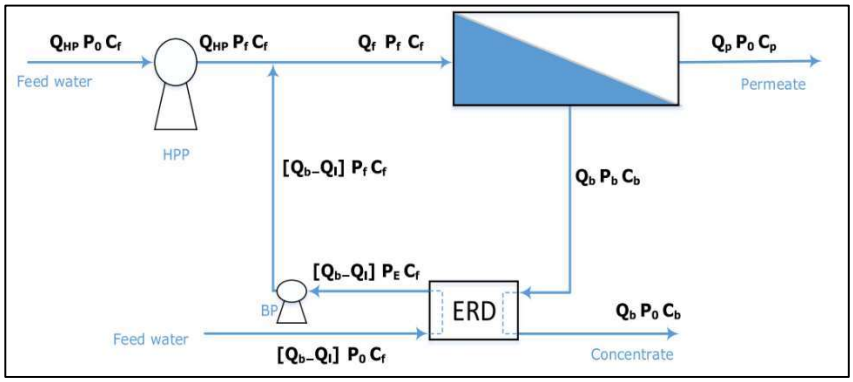

Figure 2.7: Single-stage RO with ERD (Karabelas et al., 2018)

The minimum SEC is the minimum amount of energy needed by the process to produce a unit of water. The minimum SEC relies on a few factors such as the salinity of the incoming feed water as well as the recovery ratio. SEC_{min} can be calculated by Equation 2.4 below.

$$SEC_{min} = \frac{R\hat{G}(C_p)+(1-R)\hat{G}(C_r)-\hat{G}(C_F)}{R} \quad \text{(Eq. 2.4)}$$

Where: $\hat{G}$ = Specific Gibbs free energy

C_p = Product stream concentration

C_R = Retentate stream concentration

C_F = Reed stream salinity

R = Ratio of recovered water

The efficiency of the desalination process can be calculated as follows:

$$\eta = \frac{SEC_{min}}{SEC} \quad \text{(Eq. 2.5)}$$

Thus by dividing the calculated SEC by the recorded actual SEC, an efficiency can be determined (Davenport et al., 2018).

2.4 Theoretical Design of a RO System

This section will describe the requirements to design a basic water treatment plant and will also include the software use to output the needed parameters for Electrical Control and Instrumentation (EC&I).

2.4.1 Source Water

Any water treatment design will start with an accurate water sample to establish which parameters need to be treated. A second important consideration will be that of the destination for the product water. The allowed water parameters will be different for that of different uses, such as domestic, recreational, industrial, agricultural etc. (DWAF, 1996). For human consumption, the South African National Standards (SANS) 241: 2015 for drinking water needs to be consulted (Petrik et al., 2017). A water sample can be taken at the source and then be analysed at a South African National Accreditation System (SANAS) laboratory in South Africa (Balfour et al., 2011).

2.4.2 Plant Modelling

The plant modelling aspect involves using mathematical equations to solve problems and output useful data that will lead to the next stage of the theoretical design process (Ahmed et al., 2019). By making use of different modelling techniques, different datasets of results will ultimately reveal the relationship between certain parameters by which good engineering

judgement could eliminate the need for unnecessary experiments. The below mathematical equations are used in the modelling of a RO plant (Ahmed et al., 2019; Kim et al., 2019, 2009):

$$Q_w = A(\Delta P - \Delta\pi) \quad \text{(Eq. 2.6)}$$

Where: Q_w = Product flow rate

ΔP = Difference in feed and product

$\Delta\pi$ = Osmotic pressure

Osmotic pressure can be calculated by using Equation 2.7:

$$\Delta\pi = n_i C R_g T \quad \text{(Eq. 2.7)}$$

Where: n_i = Number of moles of species

R_g = Universal gas constant 0.082 kg.m^2/h^2.K

T = Incoming feed water temperature

The recovery ratio of the system will be represented by, K, that can be calculated by using Equation 2.8:

$$K = \frac{Q_p}{Q_f} \quad \text{(Eq. 2.8)}$$

Where: Q_p = Product flow leaving the system

Q_f = Feed flow entering the system

When the TDS in the feed flow increases, at the same given temperature, the product flow will decrease because the system needs to perform more work to deal with the higher TDS. This will effectively mean that the recovery ratio will decrease (Nisan et al., 2005).

The theoretical calculation of the SEC for an RO can be calculated by using Equation 2.9 (Assad et al., 2020):

$$SEC = \frac{E_{bp}+E_{hp}+E_{sp}}{Q_p} \quad \text{(Eq. 2.9)}$$

Where: Q_p = Product flow leaving the system

E_{bp} = Booster pump energy

E_{hp} = High pressure pump energy

E_{sp} = Supply pump energy

The product flux of the membranes can be calculated with the following equation 2.10 below:

$$J_v = \frac{Q_p}{A} \quad \text{(Eq. 2.10)}$$

Where: A = Surface area of the membrane that is in contact with the product water

Temperature also plays a vital role in the design of such a RO system and thus a Temperature Correction Factor (TCF) needs to be calculated so that it can be incorporated into the design. The TCF can be multiplied with the Transmembrane Pressure (TMP) to normalize the TMP at different temperatures (Gilabert Oriol et al., 2013). The TCF can be calculated by using Equation 2.11 below (Sarai Atab et al., 2016):

$$TCF = e^{\left[\frac{E_m}{R}\left(\frac{1}{273} - \frac{1}{298}\right)\right]} \quad \text{(Eq. 2.11)}$$

Where: E_m = Membrane activation energy

R = Gas constant

T = Temperature

The amount of salt rejected, R_s, by the RO can be calculated by using Equation 2.12 below:

$$R_s = 1 - \frac{TDS_p}{TDS_f} \quad \text{(Eq. 2.12)}$$

Total mass balance can be calculated by using Equation 2.13 below (NCUBE and INAMBAO, 2021):

$$Q_f C_f = Q_p C_p - Q_r C_r \quad \text{(Eq. 2.13)}$$

Where: Q_f = Feed flow

C_f = Mass concentration of the rejected salts in the feed flow

Q_p = Product flow

C_p = Mass concentration of the rejected salts in the product flow

Q_r = Reject flow

C_r = Mass concentration of the rejected salts in the rejected flow

Product water flow can be calculated by using Equations 2.14 and 2.15 below (Ncube and Inambao, 2021):

$$Q_p = Q_f - Q_r \quad \text{(Eq. 2.14)}$$

$$Q_p = n_i W \int_0^L J_v dz \quad \text{(Eq. 2.15)}$$

Where: Q_p = Product water flow rate

n_i = Number of membrane leaves

L = Length of RO module

W = Width of RO module

2.4.3 Software Modelling

The above formulae found under heading 2.4.2 Plant Modelling, forms the theoretical background of software modelling packages, such as WAVE (Ncube and Inambao, 2021). Software modelling packages are used to simulate a plant design based on the user-input feed characteristics. Based on the input characteristics, WAVE generates an output report that governs the final plant design.

The report will contain information such as required input pressure, expected output pressures, number of membranes (based on user membrane input selection), fresh product flow and brine flow amongst others. From the required pressure and flow, pumps selection can be facilitated and thus the energy requirement can be determined.

2.4.4 Energy Consumption Forecast

An energy consumption forecast can be made based on the amount of electrical equipment, their associated sizes and the duration of operation for each piece of equipment. Based on the energy consumption needed, the power source can be selected and sized. Energy consumption for each piece of equipment can be calculated by using Equation 2.16 below:

$$E = P\ x\ t \qquad \text{(Eq. 2.16)}$$

Where: E = Energy in Watt-hours

P = Power in Watts

t = Time in hours

The total energy consumption can then be calculated by adding all of the individual energy consumptions together using Equation 2.17:

$$E_T = E_1 + E_2 + E_3 \ldots \qquad \text{(Eq. 2.17)}$$

Energy consumption must not be confused with the installed power. The installed power does not include a time function and is merely the power rating of the equipment. The peak load can be calculated by adding all of the electrical equipment that will be in operation at the same time together. Peak load may only happen once or twice a day when the duty of electrical equipment overlaps, and will not be a continuous load, but only temporary. The equipment start-up type such as DOL, VFD, Star-Delta etc. needs to be considered as the start-up current will vary with each of the above starting methods. The selected power source needs to be sufficiently sized

to handle the equipment during a peak load with their method of start, although only for small bursts of time.

A feasibility comparison can be made against the increased capital needed for a start-up method such as a VSD in comparison to a DOL starter where the power source and cables can be resized and possibly sized smaller due to lower start-up currents.

2.5 Renewable Energy

Renewable energy can be described as energy that can be harvested from natural sources that can regenerate at a faster rate than it is consumed. Renewable energy sources are green sources that do not have an impact on climate or environment and produce little greenhouse gasses (Kim and Park, 2022). Sources of renewable energy include solar energy, wind energy, geothermal energy, hydropower, ocean-energy and bioenergy. Each of these sources can be sub categorized into one or more subcategories.

Solar energy can be harvested through solar-PV panels, utilising sunlight, or through concentrating the solar through mirrors, utilising solar radiation to heat up different mediums where heat energy is required to drive a sub process, such as a boiler.

Wind energy utilises the kinetic energy stored in the wind, to mechanically turn a turbine with blades that in turn generate electricity. These turbines can be onshore or offshore where the windspeeds are adequate to turn the mechanical turbine blades.

Hydropower energy utilizes the energy stored in moving water to turn a turbine that will in turn generate power. Hydropower can be generated by a river where water continuously flows through a turbine, or in a dam setup where the water flows from a higher elevation to a lower elevation passing through a turbine. This setup can also be seen as a large battery by storing surplus energy. Surplus generated electricity from another source ‘A’ is used to pump the water back to the top elevated dam, to be moved down to the lower elevated dam, when the peak electricity demand is high and cannot be met by the source ‘A’. Hydropower can be influenced by seasonal rainfall and droughts, but despite the external influences, hydropower is still the largest contributor of renewable energy worldwide (Rahman et al., 2022).

Bioenergy is created from various organic materials such as wood, plant materials, manure etc. for heat and energy production. By burning these materials, also know as biomass, greenhouse gasses are released, but not nearly comparabile to the greenhouse gasses created by burning fossil fuels such as coal (REN21, 2020).

For the purposes of this dissertation, solar energy will be considered, as this source of energy is mostly available in South Africa (Jain and Jain, 2017). Solar energy will be further discussed in the next heading.

2.5.1 Solar Energy

Energy from the sun is readily available and has the most energy potential out of all the possible energy sources. Perez and Perez, 2009 indicates that the yearly available energy from the sun is around 23 000 TWy whereas the total energy consumption for the whole world per year for 2009 was around 16 TWy. Wind is in second place with 25 – 70 TWy per year. From this it is evident that solar is the most prominent and available renewable energy source with the capability of supplying the whole world with enough renewable power year after year.

Although solar is readily available, solar-PV panels are needed to convert this solar energy into electricity. Solar panels are very inefficient with a confirmed efficiency of 9 % at 800 W/m^2 in 2014 by Hamou et al., 2014, to 28.8% according to Inganäs and Sundström, 2016. This will confirm that from a large surface area exposed to solar radiation, a small amount of electricity can be generated. This will translate to a significantly large piece of land that will be needed to house a significant number of solar panels so that a fair amount of power can be generated. It can be assumed that space will often be a problem when solar energy is selected to be the power source.

Solar-PV panels generate electricity from solar power through utilizing the solar irradiance from the sun. Solar irradiance can be broadly defined as the light energy from the sun that covers a square meter of surface area, thus making the unit self-explanatory as W/m^2. The sunlight, composed as photons, will strike a solar-PV panel which is made up of PV cells. The cells consist of a semiconductor material which absorbs the sunlight and releases electrons from the material's atoms. These electrons carry a negative charge that flows from the back to the front (surface) of the cell, creating a potential difference (Inganäs and Sundström, 2016). Fig 2.8 is a representation of how sunlight is converted to electricity through a PV cell.

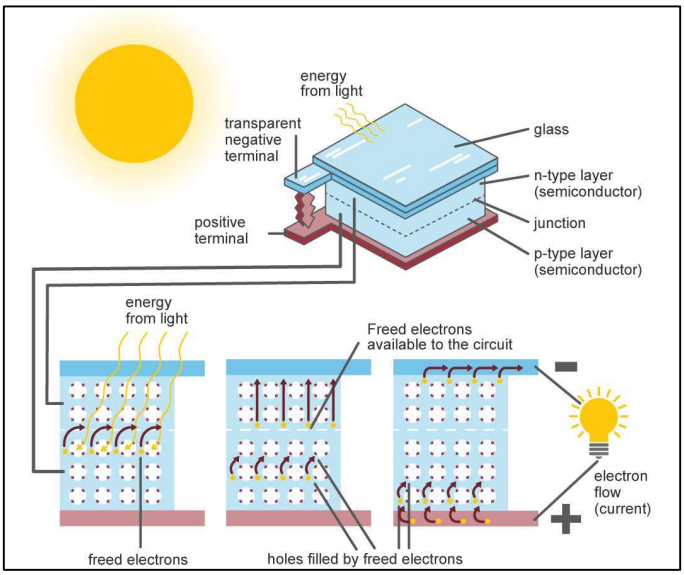

Figure 2.8: Solar PV energy conversion (EIA, 2020).

2.6 Theoretical Design of a Solar System

The most important factor to consider when designing a solar power generation plant is the available solar irradiance at the planned location of the solar plant as well as the electrical load that needs to be powered, or desired solar plant output (Al-Najideen and Alrwashdeh, 2017). Once the solar availability and electrical load has been established, the next step would be to establish a good estimation on the number of solar panels that will be needed to power the electrical load. This number could vary as the solar panels are available in different energy outputs, but with a different dimension. Typically, the higher the energy output, the larger the panel. This could lead to a space constraint as the number of solar panels needed might exceed the available mounting space of these solar panels.

If the electrical load and panel estimation has been conducted, the inverter(s) can be sized and selected. The inverter selection will depend on the electrical load and electrical system's characteristics, for example a three-phase or single-phase electrical supply configuration. The inverter will be sized to handle the electrical demand as well as the demand during peak times. It is therefore good practice to install a power logger for a week at the point of current supply so that an energy profile can be recorded to assist in selecting an inverter to cope with peak demands. The inverter and the solar panels will have to be carefully selected to be compatible with each other. The DC inputs on the inverter have certain specifications which the DC input voltage and current must adhere to. Failure to comply with this could lead to equipment failure and serious injury or even death.

2.6.1 Inverter

The heart of a solar system can be described as an inverter. This is the piece of equipment responsible for converting the DC power from the solar-PV panels into useable AC power that is outputted from the inverter. Many different types of inverters exist from grid-tied inverters and hybrid inverters, to off-grid inverters. Each type has their own strengths and weaknesses (Vairavasundaram et al., 2021). The hybrid inverter is the most versatile inverter which allows multiple configurations for keeping the power on. The hybrid inverter can supply the load from solar-PV panels, if there is enough solar power available at the time. Excess solar power can be used to charge batteries or to power other non-essential equipment. The hybrid inverter can also power the loads with a combination of battery and solar power (Subramaniam et al., 2020). Inverters can be used in a parallel configuration to add more capacity. Three single-phase inverters can be used together to form a three phase system if the inverter allows for such communication and capability (Sastry et al., 2014). Fig 2.9 is a representation of such a configuration where single phase inverters are chained together to form a three-phase power system.

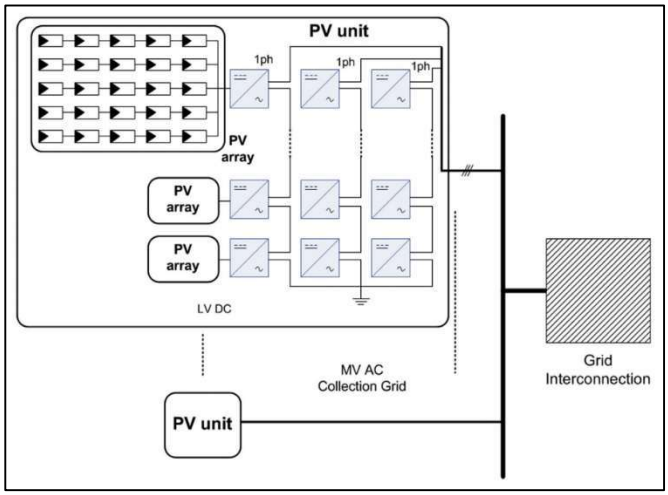

Figure 2.9: Solar-PV panels and single-phase inverter configuration (Sastry et al., 2014)

The inverter(s) size is usually calculated using one (1) of two (2) different methods. The first method involves sizing the inverter to match the amount of solar power installed by adding all of the installed PV panel wattage rating together. For example, if 12 x 500 W of solar-PV panels are installed, the inverter size is matched as close as possible to 6000 W. The second method is to downsize the inverter by 30 % in comparison with the installed solar power. Thus, for 6000 W of installed solar, the inverter will be as close as possible to 4200 W. This is due to the irradiance levels that rarely reach the Standard Test Conditions (STC) of the installed solar panels. By downsizing the inverter, a capital saving is possible. Equations 2.18 and 2.19 below are a representation of the two sizing methods mentioned above (Chen et al., 2013).

Method one:

$$P_{inv,nom} \approx P_{PV,nom} \quad \text{(Eq. 2.18)}$$

Method two:

$$P_{inv,nom} = (0{,}7) * P_{PV,nom} \quad \text{(Eq. 2.19)}$$

2.6.2 Solar-PV Panels

The basic configuration of a solar-PV panel consists of multiple solar cells that are stringed together in a series and parallel configuration as seen in Fig 2.10.

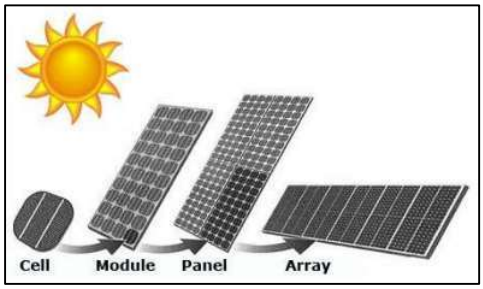

Figure 2.10: Solar-PV array configuration (Vega, 2019)

The total number of panels needed will be an addition of the number of panels for each string that will be connected to each of the inverters. The maximum string size per inverter can be calculated using Equations 2.20 and 2.21 below. This equation consists of the maximum permissible voltage input on the Maximum Power Point Tracker (MPPT) input on the inverter divided by the open circuit voltage of the selected panel that has been adjusted to compensate for the lowest expected temperature for the location of the installation (Vega, 2019).

$$Max\ String\ Size = \frac{V_{max,Inverter}}{V_{max,module}} \quad \text{(Eq. 2.20)}$$

$$V_{max,module} = V_{OC}\ x\ \left(1 + (T_{min} - T_{STC})\ x\ (Tk_{VOC}/100)\right) \quad \text{(Eq. 2.21)}$$

where: $V_{max,module}$ = Maximum MPPT allowable voltage input on the inverter

V_{OC} = Open circuit voltage – solar-PV panel

T_{min} = Minimum temperature at installation location (°C)

T_{STC} = Temperature at STC, 25°C

Tk_{VOC} = Current voltage temperature coefficient (%/°C)

The minimum string size needs to be calculated as the MPPT input on the inverter has a minimum operating voltage range for the inverter to start operation. The minimum operating string size per inverter can be calculated by using Equations 2.22 and 2.23 below (Vega, 2019):

$$Min\ String\ Size = \frac{V_{min,Inverter}}{V_{min,module}} \quad \text{(Eq. 2.22)}$$

$$V_{min,module} = V_{mp}\ x\ \left(1 + \left((T_{max} + T_{add} - T_{STC})\ x\ (Tk_{VMP}/100)\right)\right) \quad \text{(Eq. 2.23)}$$

where: $V_{min,module}$ = Minimum MPPT allowable voltage input on the inverter

V_{mp} = Rated module max voltage

T_{max} = Maximum temperature at installation location (°C)

T_{add} = +35°C – roof mounted parallel, +30°C – roof mounted rack mounted, +25°C – ground/pole mounted

Tk_{VMP} = Module temperature coefficient (%/°C)

The number of panels per inverter needs to be selected between the minimum string size and the maximum string size per inverter. The total number of panels can be calculated by using Equation 2.24 below, where the number of inverters needed will be multiplied by the number

of strings accepted by the inverter, and then multiplied by the number of panels selected between the minimum and maximum string size.

$$Total\ PV\ Panel\ amount = N_{inv}\ x\ N_{strings}\ x\ N_{panels} \quad \text{(Eq. 2.24)}$$

2.7 Smart Metering

Smart metering is exactly what the name suggests. It is the smart and advanced way of measuring energy usage. Smart meters boast the capability of being tamper proof, with real-time power measurements with an audit trail of logged time events. These meters can be directional with an import and export function of excess energy, from a source such as a solar-PV plant. The smart meter has remote communication abilities by which the managing partner of such a device can update the tariffs and information on the device, this can allow for accurate billing for using electricity within the peak time and off-peak time slots. Smart meters have the capability to measure grid, generator and Energy Storage Systems (ESS) such as a solar-PV plant (Rezaeimozafar et al., 2022).

Smart metering can be used in conjunction with other plant equipment to evaluate the overall performance and efficiency of the equipment at hand. By comparing the energy usage from the smart meter with the final treated water from a water treatment plant, one could ultimately determine the cost and efficiency of such a water treatment plant.

2.8 Chapter Summary

This chapter presented the various methods employed in water purification including membrane processes. One of the more commonly employed membrane processes is desalination, which can be applied to areas abundant in seawater. Desalination operates according to the principles governing RO, in which pressure is applied to drive water across a membrane, leaving the impurities behind. Typical pre-treatment includes additional membrane processes such as UF. Critical mechanical and electrical components of desalination include high-pressure pumps, membranes, and post-treatment. Due to the high energy attributed to desalination plants, energy efficiency techniques should be investigated and applied. The effect of applying energy efficiency techniques can be investigated by first modelling the plant's expected output before application of energy using a software such as WAVE. The output of required equipment can then facilitate the generation of an energy consumption forecast. This forecast can be used to investigate renewable energy sources, and their impact on its reduction.

3. Methodology

3.1 Introduction

In order to achieve the aims and objectives of this dissertation as set out in in the first chapter, a 1 ML/day SWRO water treatment plant will be modelled using WAVE software, freeware from creator DuPont, that was introduced in the second chapter. The WAVE software incorporates Equations 2.1 to 2.15 to output the needed information in the summary report. The input parameters for the model will be governed by characteristics of seawater. The outputs of the model will determine the mechanical requirements from which a mechanical selection, such as pumps, compressors, etc., can be made. From the mechanical design and selection, the electrical requirements will follow. Once all of the mechanical selections have been made, the total electrical energy requirement will be calculated using the power calculations from section 2.4.4. From the electrical demand, the energy usage can be calculated, based on the runtime of the plant. The theoretical calculated energy will then be compared to the actual energy consumption, obtained from the smart energy meter. From the peak electrical demand and energy requirement, a solar energy solution will be investigated to power the 1 ML/day SWRO. The results and findings will be discussed in the fourth chapter.

3.2 WAVE Design

The WAVE design commences with selecting the feedwater as seawater and the quality, Salt Density Index (SDI) < 2.5, and specifying the product flow to be 1 ML/day. The pre-treatment has been selected to be of a UF type, followed by an RO process which will ensure the product water quality. The design is done based on an average feed water temperature of 15^{o}C. After inputting the required parameters, WAVE calculates a summary report based on the equipment needed to perform according to the inputs. The summary report includes the UF information needed for the necessary design of the pre-treatment section as well as the SWRO information needed to design the RO section. The summary report will include the necessary flows and pressures to overcome elements such as friction and to stay within design parameters such as velocity in pipes etc. From the summary report for the pre-filtration and SWRO, a mass balance can then be created to avail the needed parameters to size the remainder of the equipment that is not part of the pre-filtration and the SWRO. The following equipment can be sized and selected from the summary report of the WAVE software by matching the flow and pressure required on the pump selection curve:

- Feed water pumps which will provide the UF pre-filtration with raw water. In this case the pumps will be submersible pumps located in the sea
- Clean-In-Place (CIP) pump that will pump and circulate the CIP chemicals through the UF membranes when planned maintenance occurs

- Backwash pump that will regularly perform a backwash by pumping a portion of the stored product water from the product tank through the UF membranes from the opposite side as suppose to the conventional flow direction to dislodge any material on the surface of the membranes
- Air compressor needed for the air scour that forms part of the backwash and membrane maintenance steps
- RO low pressure pump that will be located before the cartridge filter. The low-pressure pump will act as the feed pump which will feed the RO plant with the necessary flow
- RO high pressure pump that will be located before membranes. The high-pressure pump will act as the booster pump to increase the pressure and thus force the water through the small orifices in the membrane

The following equipment can be sized and selected from mass balance calculations that have been performed based on the required output with the incorporated requirements from the summary report of the WAVE software:

- Final discharge product pump can be selected based on the mass balance that will ensure the correct flow to cope with the SWRO delivery as well as the correct delivery pressure to overcome any downstream pressure head or friction

Other equipment:

- Air compressor needed for the operation of the pneumatic actuated valves. These valves will ensure that the water is flowing in the right direction depending on the process or step of the plant. The air compressor will also be utilised in any purging or backwashing functions as deemed necessary by the control philosophy

3.3 Energy Consumption

To minimise the error in equipment run time such as compressors and backwash pumps, the total installed power will be multiplied with an hourly utilisation percentage to determine the energy consumption as per Equation 2.16. The total actual power consumption will be divided by the total product flow to determine an energy consumption per unit of product water.

The installed power is the sum of all powers pertaining to the installed equipment. The actual consumed power is estimated by applying the percentage daily consumption to the relevant equipment's installed power and then adding it all together. Once the total installed power is determined as well as the total actual consumption, these values can be divided by the product flow rate in order to determine the total installed power per cubic meter of product water produced, and the total actual power consumption per cubic meter of product water produced.

To establish the real power consumption of the designed plant, the smart meter from the municipality will provide the real-time power usage for the complete water purification plant from the seawater inlet to the distribution into the municipal network. The captured plant data will be from the final product water meter that totalises the flow into the municipal network. The municipal invoice will contain the power usage and the date range. This will be matched with the totalised flow from the same date range. The total power consumed will be divided by the total product water pumped into the municipal network.

The designed plant will be located in Port Alfred, South Africa and will serve as a drought relief project for the town. From the literature review, it was evident that solar energy is one of the most available renewable energy sources in South Africa. For the purposes of this dissertation solar renewable energy will be investigated to power the above plant during the day. Battery storage will be needed to operate the plant during the night hours with the absence of solar. Battery storage for this solution was not considered as the cost would be astronomical.

From the plant design, the total power and energy usage will be determined. From these calculations, Equations 2.18 to 2.23 will be utilized to design and size the number of inverters and solar panels needed to power the designed water treatment plant. Once the number of solar panels have been calculated, the total area can be calculated that the PV panels will occupy. The solar panels will be installed at 30 degrees and grouped together in rows. Row spacing will need to be calculated to avoid shading on groups of PV panels and thus maximise the efficiency. Based on the area needed, the practicality of powering such a plant from solar energy will be discussed.

3.4 Chapter Summary

This chapter presented the theoretical design of an existing 1 ML/day desalination plant, using the modelling software WAVE. The energy consumption associated with the theoretical plant was calculated based on the equipment required as guided by the WAVE output. This was then compared to the actual power consumption of the desalination plant, as measured by the municipality's smart meter.

4. Results and Discussion

4.1 Introduction

The output of the WAVE model of the existing desalination plant was consulted in order to select the equipment required. The equipment was selected and the respective power consumptions were noted. The energy recovery techniques installed in the existing desalination plant were then noted, as these are not specifically identified in the WAVE report. The theoretical energy consumption of the plant was determined using the selected equipment as governed by the WAVE report. This was then compared to the actual energy consumption of the existing desalination plant, as measured by the municipality's smart meter. The application of solar power to the existing desalination plant was then investigated through the determination of the space that would be required, as well as the number of panels.

The WAVE summary report for both the UF and the RO can be found in Appendix A. The WAVE report is limited to the equipment required to achieve the desalination targets. It does not specify any energy recovery techniques to be employed as this depends largely on plant configuration, operational requirements, location, and availability of specialist support should it be required.

4.2 Equipment Selection

The equipment was selected based on the WAVE summary report and the mass balance calculation. Based on the timeline of the project being an emergency drought relief project, some equipment was selected either below or above the required parameters due to availability and lead times of selected equipment.

Feed Water Pump:

The WAVE summary report calculated the feed water requirement to be as close as possible to 136 m^3/h at 3.20 bar pressure. Based on the pump supplier's pump curve, and comparing this to the required flow and pressure, a pump selection was made. An SP650-2A was selected with a delivery of 140 m^3/h at 3.50 bar. The pump was coupled with a VFD to ensure a smooth energy delivery at maximum efficiency and performance. The above-mentioned pump has a power rating of 18.50 kW.

CIP Pump:

The WAVE summary report calculated the CIP pumping capacity to be at least 15 m^3/h at 2.50 bar. Comparing the required pressure and flow with the supplier's pump curve, a selection was made. The selected pump has a power rating of 7.50 kW.

Backwash Pump:

The WAVE summary report calculated the backwash pump to have a duty of at least 77 m^3/h at 25 m head, or 2.50 bar delivery pressure. The selected pump can deliver 78 m^3/h at a head of 22.80 m or 2.28 bar delivery pressure. The selected pump's power rating is 9.50 kW.

UF Air Compressor:

The air compressor for the UF is mainly for the opening of pneumatic actuated valves during normal operation. It is also used for the air scour function during a backwash cycle. The WAVE summary report calculated the air flow based on the membrane types, feed flow, feedwater type and thus the number of backwashes needed for the membranes and recovery rate to perform as designed. The amount of airflow required was reported as 120 Nm^3/h at 0.75 bar pressure. By consulting the compressor catalogue from the manufacturer, a rotary screw compressor of 5.50 kW was selected with a pressurised air receiver capacity of 750 L that can deliver a duty of 0.67 m^3/min at 10 bar.

RO Low Pressure Feed Pump:

The WAVE summary report, as indicated in Appendix A, requires the SWRO's low pressure feed pump to have a capacity of at least 111.10 m^3/h at 0 bar pressure. The wave report does not include the addition of a high flow cartridge filter between the low-pressure feed pump and the high-pressure booster pump, thus the design pressure needs to be adjusted for the low pressure pump to overcome the backpressure from the cartridge filter. Due to timelines and availability, the low-pressure pump was selected to have a duty of 90 m^3/h at 3.50 bar. The duty flow for this pump is below the suggested flow from the WAVE report and thus the end flow could be affected, however for the data gathering of this dissertation, the energy usage per water unit will stay relative. The power rating for this pump is 22 kW and will be controlled by a VFD to increase the efficiency and minimize start-up demand from the supply.

RO High Pressure Booster Pumps:

The WAVE summary report, as indicated in Appendix A, suggests that the water pressure needs to be increased to 63.90 bar at a flowrate of 110.80 m^3/h. This will allow 45 % of the intake water to be purified and the remaining 55 % to be rejected as brine flow. Due to the timelines and availability, two high-pressure pumps were used in tandem to achieve the required pressures. The first high-pressure pump was selected at 45 m^3/h at 50.10 bar with a power rating of 120 kW. This pump was controlled by a VFD and was responsible for feeding the water from the low-pressure feed pump into the SWRO membranes. The second booster pump was selected at 55 m^3/h at 3.50 bar with a power rating of 11 kW. The booster pump was controlled by a VFD and was responsible for boosting the discharge water from the ERD.

Discharge Water Pump

The discharge water pump was responsible for delivering water from the SWRO product tank into the municipal network. The discharge pump was selected at 45 m^3/h at 3 bar. Two of these pumps will operate in a duty rotate configuration to ensure productivity. Each of these pumps were rated at 30 kW and were controlled by a soft starter.

RO Air Compressor

The SWRO air compressor will be dedicated to servicing the pneumatic valves for the water purification plant. The compressor was selected at 1.50 kW.

Dosing Pumps

Dosing pumps were selected from the mass balance sheet based on the amount of chemical dosing required. These pumps were small single-phase pumps ranging from 6 – 50 L/hour. The energy requirement for these pumps was negligible.

4.3 Energy Efficiency Through System Automation

Other equipment was required to ensure the overall efficient operation of the water purification plant. This equipment may not have contributed directly to the product water but was necessary for the operation as a whole. These items include air-conditioning for the electrical Motor Control Centre (MCC), area lighting for security and night-time operations as well as the control transformer responsible for stepping down the voltage for the control elements such as the HMI and the PLC.

The designed UF and RO water purification plant are controlled by a programmable logic controller that considers many feedback parameters from the field. The feedback parameters include pressure sensors before and after pumps and filters, mag-flow meters, free-chlorine analyser, conductivity analyser and a pH analyser.

Pressure sensors are used to automatically trigger any backwash needed when the potential difference over the filters achieve and adjustable setpoint on the Human Machine Interface (HMI). The high-pressure pump is controlled on a pressure setpoint in conjunction with a VFD to ensure the correct operation of the RO membranes. The pressure differential over the membrane stages is used to trigger a CIP event. This will allow an operator to CIP the membranes and get rid of any scaling on the membranes. This will allow the system to produce the best quality water with minimal energy wastage without having to overcome unnecessary pressure in the system due to buildup in filters or scaling on the membranes.

Mag-Flow meters are used to control the feed pumps to ensure a constant flow into the system. The mag flow meter will be provided with a flow setpoint from the HMI. The PLC will utilise a Proportional and Integral Controller (PI) to control the VFD to ensure that the pump outputs

the required setpoint flow needed. The ERD utilizes a PI controller and HMI setpoint to ensure the correct amount of water is returned to minimize the effort from the primary high-pressure pump.

The discharge water pumps are responsible for pumping the RO permeate water into the municipal network. These pumps are sized to perform at maximum flow and pressure to overcome the municipal pressure. These pumps are controlled with soft starters to minimise the startup current to reduce strain on the electricity provider.

Free chlorine analyser will ensure that the chlorinated water is at the correct levels not to damage the membranes. pH and conductivity analysers ensure that the produced water is within the SANS241 specification.

4.4 Theoretical Energy Consumption

Table 4.1 includes all the equipment, their respective power ratings and their utilisation percentage as calculated in Appendix B, in order to estimate a total combined energy.

Table 4.1: Equipment and associated power ratings and consumption

Equipment	Power Rating (kW)	Percentage Utilisation Per Hour (%)	Actual Theoretical Energy Usage Per Hour (kWh)
UF Feed Pump	18.5	95%	17.58
CIP Pump	7.5	8%	0.60
Backwash Pump	9.5	3%	0.29
UF Compressor	5.5	20%	1.10
RO Low Feed	22	100%	22.00
High Pressure 1	120	99%	118.80
High Pressure 2	11	99%	10.89
RO Compressor	1.5	10%	0.15
Control	1	100%	1.00
Lights	4	50%	2.00
Aircon	11	100%	11.00
Discharge Pump Set	30	100%	30.00
Totals	241.5		215.40

The total theoretical design energy usage was calculated to be 215.40 kWh and from the WAVE design report, the 1 ML/day capacity equates to 45 m^3/h. By dividing the hourly energy usage by the hourly water purification and delivery rate, the energy consumption per unit of water can be calculated. Thus, 215.40 kWh/45m^3 will equate to 4.79 kWh of energy consumption for every cubic meter of product water produced. This is the theoretical design calculation and will be compared to the actual data recorded.

The actual design did not take into consideration the duty points at which the pumps operated at, and thus the calculation was made based on the full power consumption of all equipment. The SWRO, which is the largest contributor of overall power consumption due to the large high-pressure pumps needed to force the saline water through the membranes, were placed on a VFD to increase the efficiency of these pumps. The high-pressure pump has a product flow setpoint which it maintains through operation. This ensures the pump consumes less power when not needed. The data from Table 4.1 has been categorised into four (4) main sections to create Table 4.2 below. Pre-filtration will include all of the equipment related to the pre-filtration, such as the feed pump and compressor. SWRO will include all of the equipment needed to operate the RO portion, including equipment such as the high-pressure pumps, RO compressor etc. The utilities section will include equipment such as security and operation lights, aircon to keep electrical equipment cool etc. The distribution section will include the distribution pump that will distribute the water from the product tank to the municipal infrastructure. From Table 4.2 and Fig 4.1, it is evident that the SWRO portion contributes to the majority of consumed energy.

Table 4.2: Grouped equipment and associated power ratings and consumption

Equipment	Power Rating (kW)	Actual Energy Usage Per Hour (kWh)	Overall Energy Consumption Contribution
Pre-Filtration	35,50	18,46	8,57%
SWRO	153	151,69	70,42%
Utilities	23	15,25	7,08%
Distribution	30	30,00	13,93%

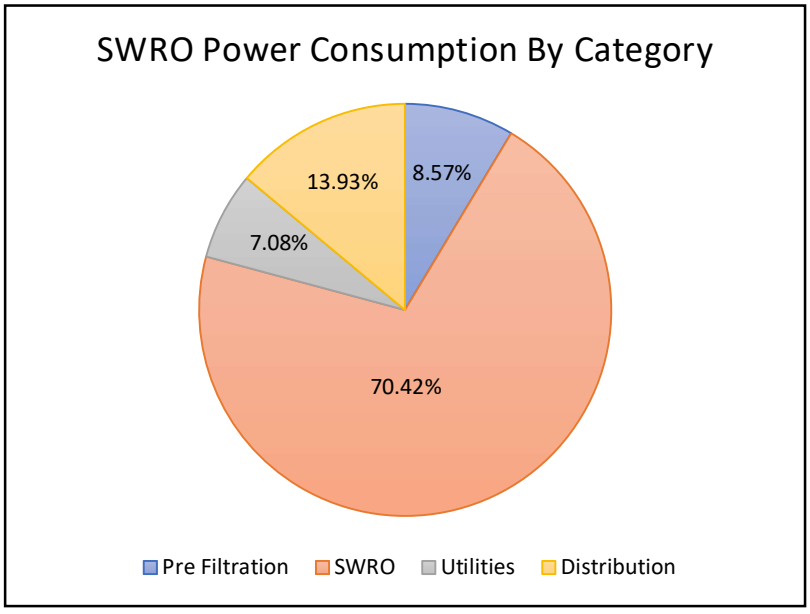

Figure 4.1: SWRO consumption by category

Considering Fig 4.1, if one is considering and including all four (4) sections of power consumption to contribute to the total comparable energy usage for such a plant, then it is

noteworthy that the energy usage per unit of water will slowly decrease as the plant size increases. This is due to the fact that some equipment sizes will not increase when the plant production output increases. The utilities section will remain the same as the plant size increases.

From the literature review it was determined that an efficient SWRO design's consumption should be anything from 3 – 6.7 kWh per cubic meter of product water produced. The variance in this number could be the fact that not all SWRO designs incorporate all of the equipment categories when that comparison is made. The above designed plant is roughly in the middle of the 3 – 6.7 kWh with 4.79 kWh but includes all of the elements from the pre-filtration to the municipal network as well as utilities. The 4.79 kWh/m^3 includes the total solution from sea to household tap. If the SWRO section was considered an element of its own, the total energy usage will look different. By only considering the SWRO section of the design, the theoretical power consumption is a mere 151.69 kWh/45m^3 which equates to 3.37 kWh per cubic meter of product water.

Although slightly smaller pumps have been selected due to global shortages, timeline and availability, the smaller pump would deliver slightly less product water but in exchange for slightly less power consumption and in turn negate any impact on the energy usage per unit of purified water.

Smart design considerations incorporating pump selection and valve configurations, has enabled the SWRO design to utilise the low-pressure feed pump for the flush and rinse operations as well. This negates the need for an extra pump to fulfil the flush and rinse functions.

4.5 Actual Power Consumption

The actual power consumption per unit of product water was calculated by dividing the actual energy consumption measured by the municipality's smart meter and the actual water usage reported from the water meter that has been produced and pumped into the municipal network. These energy consumption readings were adapted from the municipal invoices found in Appendix C and formulated in Table 4.3. The water meter readings were matched with the same date range from the municipal invoice. Table 4.3 was formulated with two full month's production data that was adapted from the raw data found in Appendix D. Table 4.3 contains two production months starting from the 19th of January 2022 until the 18th of March 2022 with their corresponding production water meter readings and month totals.

Table 4.3: SWRO actual production data by date

Date	Production (m^3)	Date	Production (m^3)
19-Jan-22	180,00	19-Feb-22	1095,00
20-Jan-22	886,00	20-Feb-22	1041,00
21-Jan-22	861,00	21-Feb-22	760,00
22-Jan-22	680,00	22-Feb-22	1051,00
23-Jan-22	1038,00	23-Feb-22	985,00
24-Jan-22	993,00	24-Feb-22	1102,00
25-Jan-22	1116,00	25-Feb-22	1067,00
26-Jan-22	739,00	26-Feb-22	848,00
27-Jan-22	1091,00	27-Feb-22	763,00
28-Jan-22	1089,00	28-Feb-22	1047,00
29-Jan-22	497,00	01-Mar-22	1117,00
30-Jan-22	976,00	02-Mar-22	1019,00
31-Jan-22	1082,00	03-Mar-22	1116,00
01-Feb-22	1104,00	04-Mar-22	1097,00
02-Feb-22	1106,00	05-Mar-22	1082,00
03-Feb-22	611,00	06-Mar-22	1061,00
04-Feb-22	282,00	07-Mar-22	859,00
05-Feb-22	657,00	08-Mar-22	666,00
06-Feb-22	886,00	09-Mar-22	676,00
07-Feb-22	1100,00	10-Mar-22	748,00
08-Feb-22	1079,00	11-Mar-22	957,00
09-Feb-22	1120,00	12-Mar-22	910,00
10-Feb-22	1086,00	13-Mar-22	968,00
11-Feb-22	1106,00	14-Mar-22	1117,00
12-Feb-22	1102,00	15-Mar-22	1094,00
13-Feb-22	996,00	16-Mar-22	1055,00
14-Feb-22	979,00	17-Mar-22	371,00
15-Feb-22	1038,00	18-Mar-22	0,00
16-Feb-22	1074,00		
17-Feb-22	1055,00		
18-Feb-22	1000,00		
Total	**28 589,00 m^3**	**Total**	**24 577,00 m^3**

Table 4.4 is the total active energy usage for the two production months. To determine the energy usage per unit of water for month one, the total energy usage for month one, 109 053.63 kWh was divided by the total production for month one, 28 589m^3. The energy consumption for the first production month was therefore found to be 3.81 kWh/m^3. Performing the same calculation for the second production month with energy consumption of 106 224.17 kWh, and a product production of 24 577 m^3, a total of 4.32 kWh/m^3 was determined. The average for the two production months therefore equated to 4.07 kWh/m^3.

Table 4.4: Active energy usage bill from the Municipality

ACTIVE ENERGY CHARGE				ACTIVE ENERGY CHARGE			
19-01-2022	to	18-02-2022		19-02-2022	to	18-03-2022	
WINTER (June, July, August)	Peak	0,00	KWh	WINTER (June, July, August)	Peak	0,00	KWh
	Standard	0,00	KWh		Standard	0,00	KWh
	Off-Peak	0,00	KWh		Off-Peak	0,00	KWh
SUMMER	Peak	17 519,93	KWh	SUMMER	Peak	15 626,59	KWh
	Standard	34 200,06	KWh		Standard	32 612,81	KWh
	Off-Peak	57 333,64	KWh		Off-Peak	57 984,78	KWh
	Total kWh	**109 053,63**			**Total kWh**	**106 224,17**	

It is evident that the calculated actual energy usage average of 4.07 kWh/m³ is lower than that of the theoretically calculated 4.79 kWh/m³. This is due to the optimisation of the control regime of the pumps and equipment as well as the incorporation of VFDs on the larger pumps which increases the efficiencies of these pumps. The larger high-pressure pumps are operating on VFDs which allow the pumps to run below their full power rating and thus consuming less energy, whereas the theoretical calculation considers the full rated power of the equipment.

By considering the difference between the theoretical and actual (0.72 kWh/m³), over the first and second month of production, the increase in energy usage would have been 20 584.08 kWh for the first production month and 17 695.44 kWh for the second month. This is an average saving of 19 139.76 kWh per month, and a total average saving of 229 677.10 kWh per year due to an optimised control system and incorporated VFDs on the larger high-pressure pumps.

4.6 Solar Power

With an average energy consumption of 215.40 kWh for 16 – 18 hours of the day when sun power is absent, approximately 3.50 MWh of storage would be required. In addition, the designed solar will have to be substantially larger to cater for the running and peak loads of the physical plant whilst also charging the 3.50 MWh battery bank with the allowable 6 – 8 hours of sun per day.

From the total installed electrical capacity, the inverters were selected followed by the solar panel design and selection. The installed power was 241.50 kW. All pumps above 5.50 kW were selected to be controlled from either a soft starter or a VFD and thus no high start-up currents were expected.

From the installed power rating of 241.50 kW, the Huawei manufacturer's catalogue was consulted, and 5 x 50 kW three-phase grid tied inverters were selected. The combined rated

output power of the five parallel installed inverters was 250 kW with the maximum power rating of 275 kW. The datasheet for the inverter can be found in Appendix E. The inverter features six MPPT inputs for the DC input side of the inverter. The solar panel manufacturer selected for this application was Canadian Solar and the panel type was of monocrystalline with an output of 545 W per panel. The number of solar panels needed was calculated by using Equations 2.20 to 2.23.

Applying Equation 2.21 to calculate the maximum voltage output from the solar panel:

$$V_{max,module} = V_{OC}\, x\, \left(1 + (T_{min} - T_{STC})\, x\, (Tk_{VOC}/100)\right)$$

$$V_{max,module} = 49.4\, x\, \left(1 + (12 - 25)\, x\, (-0.27/100)\right)$$

$V_{max,module} = 51.13$ V

Applying Equation 2.20 to calculate the maximum number of panels that the inverter can accept based on the Vmax, module calculation.

$$Max\ String\ Size = \frac{V_{max,Inverter}}{V_{max,module}}$$

$$Max\ String\ Size = \frac{1000\ V}{51.13\ V}$$

$Max\ String\ Size = 19.56 \approx 19$ Panels

Applying Equation 2.23 to calculate the maximum voltage output from the solar panel:

$$V_{min,module} = V_{mp}\, x\, \left(1 + \left((T_{max} + T_{add} - T_{STC})\, x\, (Tk_{VMP}/100)\right)\right)$$

$$V_{min,module} = 49.4\, x\, \left(1 + \left((26 + 25 - 25)\, x\, (-0.27/100)\right)\right)$$

$V_{min,module} = 45.93$ V

Applying Equation 2.22 to calculate the minimum number of panels that the inverter can accept based on the Vmax, module calculation.

$$Min\ String\ Size = \frac{V_{min,Inverter}}{V_{min,module}}$$

$$Min\ String\ Size = \frac{200}{45.93}$$

$Min\ String\ Size = 4.35 \approx 5$

The inverter features six (6) MPPT inputs, thus the number of maximum panels per MPPT could be multiplied by six (6). The total amount of panels per inverter was therefore found to be 19 x 6 = 114 solar-PV panels. This totalled 62 130 W of installed solar power per inverter. The 114 solar-PV panels per inverter, were multiplied by the total number of inverters. The

total number of solar panels required across the five (5) inverters was therefore found to be 114 x 5 = 570 solar-PV panels. The total installed solar power was therefore found to be 570 x 545 W = 310.65 kW.

Solar panels were grouped into groups of 60 panels. There were ten (10) rows in the X-axis, featuring three (3) rows. These groups of 30 panels were replicated 19 times to allow for 570 PV panels. Fig 4.2 is a representation of the group layout.

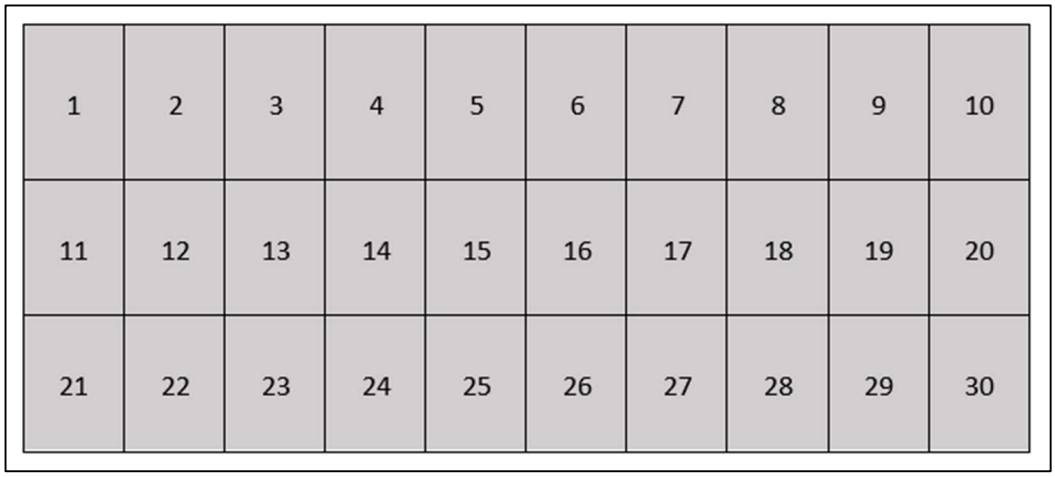

Figure 4.2: PV panel group layout

The total area that each group occupied with the group of panels tilted at 30° was calculated. The COS function at 30° determined the X-axis occupied. The X-axis was multiplied by the length of ten (10) panels to determine the area occupied by the group.

Fig 4.3 is a representation of the dimensions and angle of the solar-PV panel group.

Applying the COS function to calculate the X-axis, was performed as follows:

COS(30°) = X-axis / 6.76

X-axis = 6.76 x COS(30°)

X-axis = 5.85 m

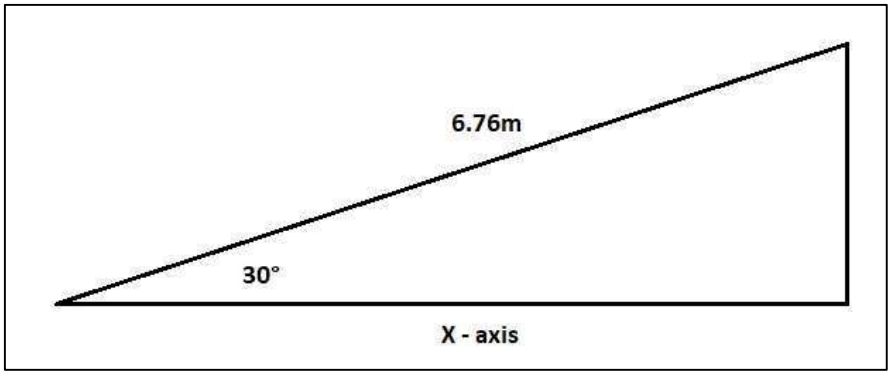

Figure 4.3: PV panel mounting layout

The width of ten (10) PV panels was calculated as 10 x 1.135 m = 11.35 m. The total area of the group was then calculated by multiplying the X-axis and the Y-axis. The total area occupied by a group of solar PV panels was found to be 5.85 m x 11.45 m = 66.40 m² per group.

The row spacing between the groups was calculated by manipulating the values in Fig 4.4 to solve for unknown *x*.

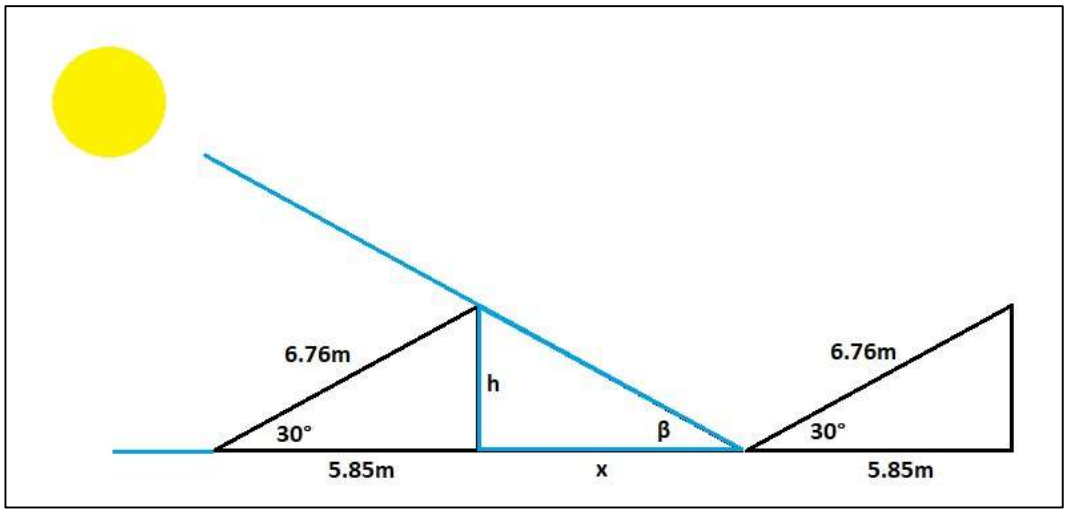

Figure 4.4: Row spacing and sun altitude angle

From Fig 4.4 and basic trigonometry, *h*, was calculated as follows:

SIN(30°) = *h*/6.76 m

h = 6.76 x SIN(30°)

h = 3.38 m

By obtaining the value for *h* and knowing the altitude angle of the sun (β), the value of *x* was calculated. The lowest value for β in Port Alfred is in June, on winter solstice with a sun rising value of 66°.

TAN(66°) = *h*/*x*

x = *h*/TAN(66°)

x = 2.25 m

The row spacing will have a length of 2.25 m and a width the same as that of the PV group, 11.45 m. The total area occupied between the two groups of PV panels was 2.25 m x 11.45 m = 25.76 m². The total area that the solar panels occupied was calculated as 19 x panel group area with the addition of 18 x row spacing area. The final occupied was therefore found to be (19 x 66.40) + (18 x 25.76) = 1725.28 m².

The calculated area roughly requires a piece of land with dimensions of 125 m x 14 m to accommodate the number of solar panels needed to power a plant of this capacity during the

daytime when solar is available. Although it is not impossible, it is highly unlikely that the amount of space required would be available for this number of required solar PV panels. It would not be practical to power such an energy intensive water purification plant from a solar-PV plant dedicated only to the water purification plant. Renewable energy will still be able to power such a water purification plant, but from dedicated renewable plants where the sources feed into the national grid. In this case, blockchain technology in energy can be investigated through smart metering to allow such a water purification plant to only allow energy usage from a renewable source.

5. Conclusions and Recommendations

5.1 Introduction

An efficient water purification plant was designed with WAVE modelling software. The theoretical energy usage was calculated by adding all of the energy consuming equipment and incorporating a theoretical daily run time of equipment. The actual energy usage was obtained from the smart metering used by the municipality. These energy consumptions were compared with one another, in order to quantify the effect of the energy recovery techniques applied to the existing desalination plant. Solar as a renewable energy was then investigated to power the existing desalination plant.

5.2 Conclusion

The theoretical energy usage was calculated to be 4.79 kWh/m³. The actual energy usage was calculated by dividing the energy usage from the municipality by the totalizer of the water flow meter from the purification plant. The actual flow was calculated to be 4.07 kWh/m³. The theoretical and actual energy usage per unit of water was then compared to industry research to satisfy the research aim of designing an efficient water purification plant. The industry standard for a SWRO plant should be between 3 and 6.70 kWh/m³. It is important to note that the actual energy usage of 4.07 kWh/m³ includes the complete process from the inlet pumps to the distribution pumps, security lighting, air-conditioning for electrical equipment etc.

The theoretical SWRO only energy usage was calculated to be 3.37 kWh/m³. Industry research fails to mention the exact processes and equipment included in the 3 – 6.70 kWh/m³ and thus the 3.37 kWh/m³ for the SWRO process and the 4.07 kWh/m³ from the total process are both noteworthy. The difference between the actual and theoretical energy consumptions was 0.72 kWh/m³ of product water. This may have been the result of efficient control methods and equipment which were selected. The 0.72 kWh/m³ saving in energy contributes to a total average saving of 19 139.76 kWh per month or 229 667.10 kWh per year. It is thus evident that by incorporating efficient starting methods as well as control methods to the electrical equipment, energy savings would be ensured. Not only can start-up currents be limited by incorporating equipment such as VFDs, but the duty point of the driven equipment can also be optimized. Pumps can ramp up and down to deliver setpoint flows and do not necessarily run at 50 Hz when not required.

The objective was to investigate the practicality of powering a 1 ML/day SWRO water purification plant with a renewable energy source. South Africa's most abundant renewable energy source is solar. Solar-PV technology was therefore investigated as the source to power a 1 ML/day SWRO water purification plant. The peak power needed was calculated by adding all of the equipment sizes together. The total power was used to determine the number of

inverters required. From the number of inverters, the number of solar panels was calculated. The total power was calculated to be 241.50 kW. It can be noted that some of the smaller equipment items, such as the CIP pump, would not run at the same time as the high-pressure pump and thus 250 kW was selected, to be the total inverter power required. This resulted in 5 x 50 kW three-phase grid tied inverters. From the inverter selection, the maximum solar panels that the MPPT DC inputs that the inverters would accept, was calculated. The widely used industry standard monocrystalline panel from Canadian Solar with a power output of 545 W was selected to perform the calculation to determine the number of solar panels that are compatible with 5 x 50 kW Huawei inverters. The total number of solar PV panels was therefore calculated to be 570. The area of each panel, alongside the angle of tilt as well as the altitude angle of the sun during a winter solstice was considered in determining the final area required to ground mount 570 solar-PV panels. The total was calculated to be 1725.28 m². This would require an area of at least 125 m x 14 m.

It was found that solar-PV technology would be able to power a 1 ML/day water purification plant, however the area required for ground mounted solar PV panels would not be practical. A small plant would require less solar-PV panels and could be practical. The capacity of an RO plant which would be practical to power from solar-PV panels, could be further investigated. By investigating smart energy meters and green energy blockchain technology, a 1 ML/day water purification plant can still be powered from solar-PV energy without the solar-PV panels being nearby. The blockchain technology could enable such a plant to run from the electrical utility grid, but only from energy from which the source is known, such as a solar-PV farm, and thus such a plant would still be powered by renewable energy.

Smart metering technology from the Municipality ensured that the energy usage specific to the water purification plant was logged. The smart energy meter, coupled with the water purification plant's flowmeters enabled the build of a database of energy usage versus water purification. Multiple flow meters installed in the water purification plant for different processes, such as backwash flow, product flow, feed flow etc. were also used to ensure that the water balancing was monitored across the plant. This also helped in ensuring that there were no leaks, and every litre of product water was optimised efficiently to save energy.

5.3 Recommendations

This work has concluded that the application of energy recovery techniques results in lower energy consumption in desalination plants, and subsequently, lower operating costs. Future work should seek to quantify the reduction applied by each energy recovery technique across a range of plant capacities. This can then be applied to theoretical models of desalination plants, to obtain a more accurate estimate of the operating conditions associated with desalination plants.

In addition, future work should look at obtaining a variety of comparison data points between the theoretical models of desalination plants, and their actual output data. This will improve understanding of the disparity between the theoretical operational data and the actual operating data, allowing designers to more accurately estimate the actual operational conditions of desalination plants.

References

Alharbi, M., Aljehani, F., N'Doye, I. & Laleg-Kirati, T.-M., 2020. Adaptive and Robust Control for Energy Efficiency Enchancement of a Solar-powered Desalination System. *IFAC-PapersOnLine,* 53(2), pp. 16543-16548.

Anand, B. et al., 2021. A review on solar photovoltaic thermal integrated desalination technologies. *Renewable and Sustainable Energy Reviews,* 141(1), p. A110787.

Boadi, N. O. et al., 2020. Safety of borehole water as an alternative drinking water source. *Scientific African,* 10(1), p. e00657.

Centre For Sustainable Systems, University of Michigan, 2020. *Wind Energy Factsheet.* [Online]
Available at: http://css.umich.edu/factsheets/wind-energy-factsheet
[Accessed 16 April 2021].

CSIR, 2016. *WIND AND SOLAR PV RESOURCE AGGREGATION STUDY FOR SOUTH AFRICA.* [Online]
Available at: https://www.csir.co.za/study-shows-abundance-wind-and-solar-resources-south-africa
[Accessed 7 May 2021].

de Wet, P., 2020. *Business Insider : South Africa.* [Online]
Available at: https://www.businessinsider.co.za/water-prices-have-increased-massively-in-south-africa-over-the-last-decade-the-reserve-bank-says-2020-10
[Accessed 07 April 2021].

Evans, J., 2012. *Pumps & Systems.* [Online]
Available at: https://www.pumpsandsystems.com/pump-efficiency-what-efficiency
[Accessed 16 April 2021].

IRENA, 2020. *IRENA: How Falling Costs Make Renewables a Cost-effective Investment.* [Online]
Available at: https://www.irena.org/newsroom/articles/2020/Jun/How-Falling-Costs-Make-Renewables-a-Cost-effective-Investment
[Accessed 07 05 2021].

Jayanthi, G., Mathumitha, N., Swathy, S. & Aaradhika, S., 2020. *Smart Monitoring and Control of Water Filtration System Using IOT.* s.l., IEEE, pp. 1-5.

Muller, R. I. & Booysen, M. J., 2014. *A Water Flow Meter for Smart Metering Applications.* Cape Town, Researchgate.

Okampo, J. & Nwulu, N., 2021. Optimisation of renewable energy powered reverse osmosis desalination systems: A state-of-the-art review. *Renewable and Sustainable Energy Reviews,* 140(1).

Pangarkar, B. L., Sane, M. G. & Guddad, M., 2011. Reverse Osmosis and Membrane Distillation for Desalination of Groundwater: A Review. *International Scholarly Research Notices,* 1(1), p. 9.

Phuangpornpitak, N. & Katejanekarn, T., 2016. Suitability analysis for implementing a renewable energy. *Energy Procedia,* 89(1), pp. 55-68.

Popescu, R. C., Fufa, M. O. M., Grumezescu, A. M. & Holban, A. M., 2017. 12: Nanostructurated membranes for the microbiological purification of drinking water. In: A. M. Grumezescu, ed. *Water Purification.* s.l.:Academic Pres, pp. 421-446.

Qin, D.-D.et al., 2019. Self-floating aerogel composed of carbon nanotubes and ultralong hydroxyapatite nanowires for highly efficient solar energy-assisted water purification. *Carbon,* 150(1), pp. 233-243.

Sola Group, 2013. *South Africa's Solar Resource Compared to the Rest of the World.* [Online] Available at: https://solagroup.co.za/news/south-africas-solar-resource-compared-to-the-rest-of-the-world/#:~:text=According%20to%20the%20South%20African,as%20South%20Africa%2C%20are%20currently
[Accessed 16 April 2021].

USAID, 2021. *South Africa: Power Africa fact Sheet.* [Online] Available at: https://www.usaid.gov/powerafrica/south-africa
[Accessed 16 April 2021].

Winter, K., 2018. *Crisis proofing South Africa's water security.* [Online] Available at: https://theconversation.com/crisis-proofing-south-africas-water-security-106261#:~:text=South%20Africa%20is%20often%20referred,the%20world%20average%20of%20860mm.
[Accessed 16 April 2021].

Zablocki, A., 2019. *EESIL Fact Sheet: Energy Storage.* [Online] Available at: https://www.eesi.org/papers/view/energy-storage-2019
[Accessed 07 05 2021].

Ahmed, F.E., Hashaikeh, R., Diabat, A., Hilal, N., 2019. Mathematical and optimization modelling in desalination: State-of-the-art and future direction. Desalination 469, 114092.

https://doi.org/10.1016/j.desal.2019.114092

Al-Karaghouli, A., Kazmerski, L.L., 2013. Energy consumption and water production cost of conventional and renewable-energy-powered desalination processes. Renew. Sustain. Energy Rev. 24, 343–356. https://doi.org/10.1016/j.rser.2012.12.064

Al-Najideen, M.I., Alrwashdeh, S.S., 2017. Design of a solar photovoltaic system to cover the electricity demand for the faculty of Engineering- Mu'tah University in Jordan. Resour. Technol. 3, 440–445. https://doi.org/10.1016/j.reffit.2017.04.005

Assad, M.E.H., Al-Shabi, M., Khaled, F., 2020. Reverse Osmosis with an energy recovery device for seawater desalinaton powered by Geothermal energy, in: In 2020 Advances in Science and Engineering Technology International Conferences (ASET). pp. 1–23.

Balfour, F., Badenhorst, H., Trollip, D., 2011. A Gap Analysis of Water Testing Laboratories in South Africa.

Bonnelye, V., Sanz, M.A., Durand, J.P., Plasse, L., Gueguen, F., Mazounie, P., 2004. Reverse osmosis on open intake seawater: Pre-treatment strategy. Desalination 167, 191–200. https://doi.org/10.1016/j.desal.2004.06.128

Brover, S., Lester, Y., Brenner, A., Sahar-Hadar, E., 2022. Optimization of ultrafiltration as pre-treatment for seawater RO desalination. Desalination 524, 115478. https://doi.org/10.1016/j.desal.2021.115478

Chen, S., Li, P., Brady, D., Lehman, B., 2013. Determining the optimum grid-connected photovoltaic inverter size. Sol. Energy 87, 96–116. https://doi.org/10.1016/j.solener.2012.09.012

Davenport, D.M., Deshmukh, A., Werber, J.R., Elimelech, M., 2018. High-Pressure Reverse Osmosis for Energy-Efficient Hypersaline Brine Desalination: Current Status, Design Considerations, and Research Needs. Environ. Sci. Technol. Lett. 5, 467–475. https://doi.org/10.1021/acs.estlett.8b00274

Duranceau, S.J., Wilder, R.J., Douglas, S.S., 2012. Guidance and recommendations for posttreatment of desalinated water. J. Am. Water Works Assoc. 104. https://doi.org/10.5942/jawwa.2012.104.0119

DWAF, D. of W. and F., 1996. South African Water Quality Guidelines: Volume 1 Domestic Use, Department of Water Affairs and Forestry.

EIA, 2020. Photovoltaics and electricity - U.S. Energy Information Administration (EIA) [WWW Document]. U.S Energy Inf. Adm. URL https://www.eia.gov/energyexplained/solar/photovoltaics-and-electricity.php (accessed

12.3.22).

Engelhardt, T., 2012. Granular Media Filtration for Water Treatment Applications. Foreign Aff. 91, 1689–1699.

Ghaffour, N., Bundschuh, J., Mahmoudi, H., Goosen, M.F.A., 2015. Renewable energy-driven desalination technologies: A comprehensive review on challenges and potential applications of integrated systems. Desalination 356, 94–114. https://doi.org/10.1016/j.desal.2014.10.024

Gilabert Oriol, G., Hassan, M., Dewisme, J., Busch, M., Garcia-Molina, V., 2013. High efficiency operation of pressurized ultrafiltration for seawater desalination based on advanced cleaning research. Ind. Eng. Chem. Res. 52, 15939–15945. https://doi.org/10.1021/ie402643z

Gude, V.G., 2011. Energy consumption and recovery in reverse osmosis. Desalin. Water Treat. 36, 239–260. https://doi.org/10.5004/dwt.2011.2534

Guirguis, M.J., 2011. Energy Recovery Devices In Seawater Reverse Osmosis Desalination Plants With Emphasis On Efficiency And Economical Analysis Of Isobaric Versus Centrifugal Devices 123.

Hamou, S., Zine, S., Abdellah, R., 2014. Efficiency of PV module under real working conditions. Energy Procedia 50, 553–558. https://doi.org/10.1016/j.egypro.2014.06.067

Inganäs, O., Sundström, V., 2016. Solar energy for electricity and fuels. Ambio 45, 15–23. https://doi.org/10.1007/s13280-015-0729-6

Jain, S., Jain, P.K., 2017. The rise of Renewable Energy implementation in South Africa. Energy Procedia 143, 721–726. https://doi.org/10.1016/j.egypro.2017.12.752

Kang, G. dong, Cao, Y. ming, 2012. Development of antifouling reverse osmosis membranes for water treatment: A review. Water Res. 46, 584–600. https://doi.org/10.1016/j.watres.2011.11.041

Karabelas, A.J., Koutsou, C.P., Kostoglou, M., Sioutopoulos, D.C., 2018. Analysis of specific energy consumption in reverse osmosis desalination processes. Desalination 431, 15–21. https://doi.org/10.1016/j.desal.2017.04.006

Kim, J., Park, K., Yang, D.R., Hong, S., 2019. A comprehensive review of energy consumption of seawater reverse osmosis desalination plants. Appl. Energy 254, 113652. https://doi.org/10.1016/j.apenergy.2019.113652

Kim, S.J., Oh, S., Lee, Y.G., Jeon, M.G., Kim, I.S., Kim, J.H., 2009. A control methodology for the feed water temperature to optimize SWRO desalination process using genetic

programming. Desalination 247, 190–199. https://doi.org/10.1016/j.desal.2008.12.024

Kim, S.K., Park, S., 2022. Impacts of renewable energy on climate vulnerability: A global perspective for energy transition in a climate adaptation framework. Sci. Total Environ. 859, 160175. https://doi.org/10.1016/j.scitotenv.2022.160175

LENNTECH, 2020. Reverse Osmosis Recovery Rate [WWW Document]. URL https://www.lenntech.com/systems/reverse-osmosis/ro/reverse-osmosis-recovery-rate.htm (accessed 4.27.22).

Maynard, E., Whapham, C., 2019. Quality and supply of water used in hospitals, Second Edi. ed, Decontamination in Hospitals and Healthcare. Elsevier Ltd. https://doi.org/10.1016/B978-0-08-102565-9.00003-0

Mito, M.T., Ma, X., Albuflasa, H., Davies, P.A., 2019. Reverse osmosis (RO) membrane desalination driven by wind and solar photovoltaic (PV) energy: State of the art and challenges for large-scale implementation. Renew. Sustain. Energy Rev. 112, 669–685. https://doi.org/10.1016/j.rser.2019.06.008

NCUBE, R., INAMBAO, F.L., 2021. Modeling, Simulation and Optimization of a Reverse Osmosis Desalination Plant. Int. J. Mech. Prod. Eng. Res. Dev. 11, 27–46.

Nisan, S., Commerçon, B., Dardour, S., 2005. A new method for the treatment of the reverse osmosis process, with preheating of the feedwater. Desalination 182, 483–495. https://doi.org/10.1016/j.desal.2005.02.041

Okampo, E.J., Nwulu, N., 2021. Optimisation of renewable energy powered reverse osmosis desalination systems: A state-of-the-art review. Renew. Sustain. Energy Rev. 140, 110712. https://doi.org/10.1016/j.rser.2021.110712

Pangarkar, B.L., Sane, M.G., Guddad, M., 2011. Reverse Osmosis and Membrane Distillation for Desalination of Groundwater: A Review. ISRN Mater. Sci. 2011, 1–9. https://doi.org/10.5402/2011/523124

Peñate, B., García-Rodríguez Lourdes, L., 2011. Energy optimisation of existing SWRO (seawater reverse osmosis) plants with ERT (energy recovery turbines): Technical and thermoeconomic assessment. Energy 36, 613–626. https://doi.org/10.1016/j.energy.2010.09.056

Perez, R., Perez, M., 2009. A Fundamental Look At Energy Reserves For The Planet. Int. Energy Agency SHC Program. Sol. Updat. 50, 4–6.

Petrik, L., Green, L., Abegunde, A.P., Zackon, M., Sanusi, C.Y., Barnes, J., 2017. Desalination and seawater quality at Green Point, Cape Town: A study on the effects of marine sewage

outfalls. S. Afr. J. Sci. 113, 1–10. https://doi.org/10.17159/sajs.2017/a0244

Qiu, T., Davies, P.A., 2012. Comparison of configurations for high-recovery inland desalination systems. Water (Switzerland) 4, 690–706. https://doi.org/10.3390/w4030690

Rahman, A., Farrok, O., Haque, M.M., 2022. Environmental impact of renewable energy source based electrical power plants: Solar, wind, hydroelectric, biomass, geothermal, tidal, ocean, and osmotic. Renew. Sustain. Energy Rev. 161, 112279. https://doi.org/10.1016/j.rser.2022.112279

REN21, 2020. Renewables 2020 Global Status Report, Global Status Report for Buildings and Construction: Towards a Zero-emission, Efficient and Resilient Buildings and Construction Sector.

Rezaeimozafar, M., Monaghan, R.F.D., Barrett, E., Duffy, M., 2022. A review of behind-the-meter energy storage systems in smart grids. Renew. Sustain. Energy Rev. 164, 112573. https://doi.org/10.1016/j.rser.2022.112573

Sarai Atab, M., Smallbone, A.J., Roskilly, A.P., 2016. An operational and economic study of a reverse osmosis desalination system for potable water and land irrigation. Desalination 397, 174–184. https://doi.org/10.1016/j.desal.2016.06.020

Sastry, J., Bakas, P., Kim, H., Wang, L., Marinopoulos, A., 2014. Evaluation of cascaded H-bridge inverter for utility-scale photovoltaic systems. Renew. Energy 69, 208–218. https://doi.org/10.1016/j.renene.2014.03.049

Schunke, A.J., Hernandez Herrera, G.A., Padhye, L., Berry, T.A., 2020. Energy Recovery in SWRO Desalination: Current Status and New Possibilities. Front. Sustain. Cities 2, 1–7. https://doi.org/10.3389/frsc.2020.00009

Subramaniam, U., Vavilapalli, S., Padmanaban, S., Blaabjerg, F., Holm-Nielsen, J.B., Almakhles, D., 2020. A hybrid PV-battery system for ON-grid and off-grid applications-controller-in-loop simulation validation. Energies 13. https://doi.org/10.3390/en13030755

Tabatabai, A., 2014. Coagulation and Ultrafiltration in Seawater Reverse Osmosis Pretreatment.

Vairavasundaram, I., Varadarajan, V., Pavankumar, P.J., Kanagavel, R.K., Ravi, L., Vairavasundaram, S., 2021. A review on small power rating pv inverter topologies and smart pv inverters. Electron. 10. https://doi.org/10.3390/electronics10111296

Vega, A.G., 2019. ScholarWorks @ UARK Designing a Solar PV System to Power a Single-Phase Distribution System.

Water-Rightgroup, 2003. How does reverse osmosis work ?

Appendices

Appendix A – WAVE Summary Report

UF Summary Report

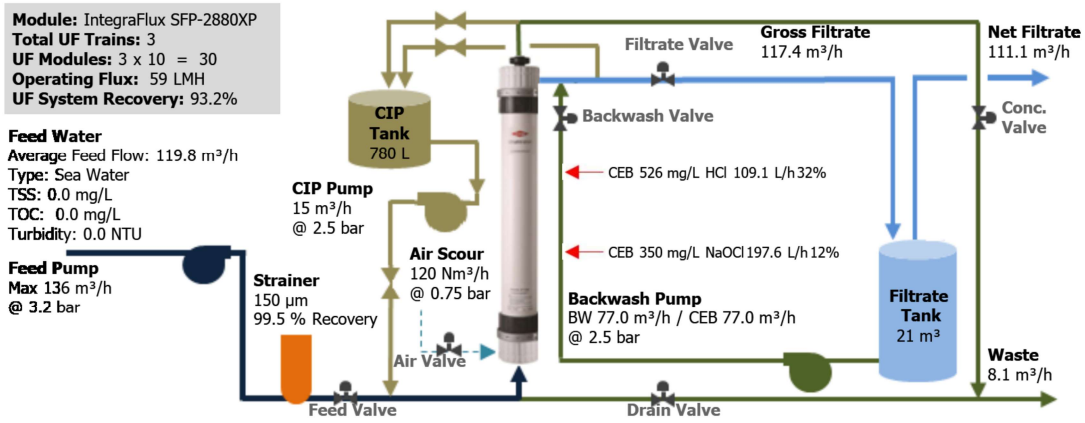

UF System Overview

Module Type		IntegraFlux SFP-2880XP			
# Trains		Online =	3	Standby =	0
				Redundant =	0
# Modules		Per Train =	10	Total =	30
System Flow Rate	(m³/h)	Gross Feed =	119.8	Net Product =	111.1
Train Flow Rate	(m³/h)	Gross Feed =	39.9	Net Product =	37.0
UF System Recovery	(%)	93.18			
TMP	(bar)	0.42 @ 15.0 °C		0.42 @ 15.0 °C	
Utility Water		Forward Flush:	Pretreated water	Backwash:	UF filtrate water
		CEB Water Source:	UF filtrate water	CIP Water Source:	UF filtrate water

UF Operating Conditions

	Duration	Interval	Flux/Flow
Filtration:	35.0 min	39.3 min	-
Instantaneous			
3 Online Trains			59 LMH
3 Total Trains			59 LMH
Average			51 LMH
Net			48 LMH
Backwash	4.3 min	39.3 min	100 LMH
Acid CEB	17.9 min	72 h	100 LMH
Alkali CEB	17.9 min	12 h	100 LMH
CIP	315.9 min	60 d	1.50 m³/h

UF Water Quality

Stream Name		Seawater - Standard Reference	
Water Type		Sea Water (15.0 - 25.0 °C)	
		Feed	**Expected UF Product Water Quality**
Temperature	(°C)	15.0	15.0
TDS	(mg/L)	35988	35988
pH		8.2	8.2

UF Design Warnings

None

RO Summary Report

RO System Flow Diagram

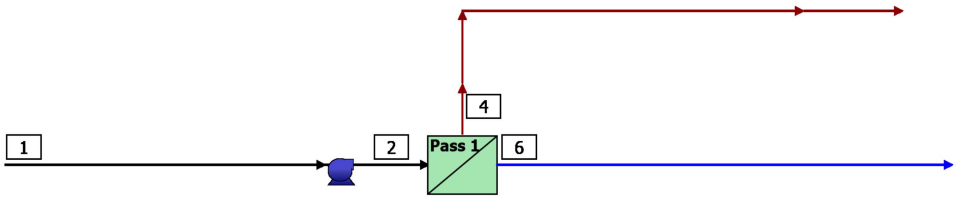

#	Description	Flow (m^3/h)	TDS (mg/L)	Pressure (bar)
1	Raw Feed to RO System	111.1	35,987	0.0
2	Net Feed to Pass 1	110.8	36,072	63.9
4	Total Concentrate from Pass 1	61.0	65,511	62.3
6	Net Product from RO System	50.0	86.64	0.0

RO System Overview

Total # of Trains	1	Online =	1	Standby =	0	RO Recovery	45.0 %
System Flow Rate	(m^3/h)	Net Feed =	111.1	Net Product =	50.0		

Pass		Pass 1
Stream Name		Seawater - Standard Reference
Water Type		Seawater With DuPont UF, SDI < 2.5
Number of Elements		78
Total Active Area	(m^2)	2899
Feed Flow per Pass	(m^3/h)	110.8
Feed TDS[a]	(mg/L)	36,072
Feed Pressure	(bar)	63.9
Flow Factor Per Stage		0.85
Permeate Flow per Pass	(m^3/h)	50.0
Pass Average flux	(LMH)	17.2
Permeate TDS[a]	(mg/L)	86.64
Pass Recovery		45.1 %
Average NDP	(bar)	27.7
Specific Energy	(kWh/m^3)	4.94
Temperature	(°C)	15.0
pH		8.2
Chemical Dose		-
RO System Recovery		45.0 %
Net RO System Recovery		45.0%

Footnotes:

[a]Total Dissolved Solids includes ions, SiO_2 and $B(OH)_3$. It does not include NH_3 and CO_2

RO Flow Table (Stage Level) - Pass 1

Stage	Elements	#PV	#Els per PV	Feed				Concentrate			Permeate			
				Feed Flow (m^3/h)	Recirc Flow (m^3/h)	Feed Press (bar)	Boost Press (bar)	Conc Flow (m^3/h)	Conc Press (bar)	Press Drop (bar)	Perm Flow (m^3/h)	Avg Flux (LMH)	Perm Press (bar)	Perm TDS (mg/L)
1	SW30HRLE-400	13	6	110.8	0.00	63.6	0.0	61.0	62.3	1.3	50.0	17.2	0.0	86.64

RO Solute Concentrations - Pass 1

Concentrations (mg/L as ion)				
		Concentrate	Permeate	
	Feed	Stage1	Stage1	Total
NH_4^+	0.00	0.00	0.00	0.00
K^+	408.4	743.2	1.30	1.30
Na^+	11,033	20,083	30.34	30.34
Mg^{+2}	1,314	2,393	0.83	0.83
Ca^{+2}	421.7	768.3	0.26	0.26
Sr^{+2}	8.14	14.82	0.01	0.01
Ba^{+2}	0.00	0.00	0.00	0.00
CO_3^{-2}	14.25	27.59	0.00	0.00
HCO_3^-	107.7	193.3	0.45	0.46
NO_3^-	0.00	0.00	0.00	0.00
F^-	1.33	2.42	0.00	0.00
Cl^-	19,807	36,055	49.99	49.99
Br^{-1}	68.85	125.3	0.26	0.26
SO_4^{-2}	2,776	5,058	0.70	0.70
PO_4^{-3}	0.00	0.00	0.00	0.00
SiO_2	1.00	1.82	0.00	0.00
Boron	4.59	8.02	0.43	0.43
CO_2	0.44	0.98	0.55	0.55
TDS[a]	35,987	65,511	86.64	86.64
Cond. µS/cm	53,427	90,181	178	178
pH	8.2	8.1	6.2	6.2

Footnotes:

[a]Total Dissolved Solids includes ions, SiO_2 and $B(OH)_3$. It does not include NH_3 and CO_2

RO Design Warnings

None

Special Comments

None

RO Flow Table (Element Level) - Pass 1

Stage	Element	Element Name	Recovery (%)	Feed Flow (m^3/h)	Feed Press (bar)	Feed TDS (mg/L)	Conc Flow (m^3/h)	Perm Flow (m^3/h)	Perm Flux (LMH)	Perm TDS (mg/L)
1	1	SW30HRLE-400	10.7	8.53	63.6	36,072	7.61	0.91	24.6	47.87
1	2	SW30HRLE-400	10.6	7.61	63.3	40,390	6.81	0.81	21.7	60.04
1	3	SW30HRLE-400	10.2	6.81	63.0	45,159	6.12	0.69	18.7	76.73
1	4	SW30HRLE-400	9.5	6.12	62.8	50,266	5.54	0.58	15.6	99.88
1	5	SW30HRLE-400	8.6	5.54	62.6	55,523	5.06	0.47	12.7	132.3
1	6	SW30HRLE-400	7.4	5.06	62.4	60,687	4.69	0.37	10.1	177.9

Footnotes:

[a]Total Dissolved Solids includes ions, SiO_2 and $B(OH)_3$. It does not include NH_3 and CO_2

RO Solubility Warnings

Warning	Pass No
Stiff & Davis Stability Index > 0	1
Anti-scalants may be required. Consult your anti-scalant manufacturer for dosing and maximum allowable system recovery.	1

RO Chemical Adjustments

	Pass 1 Feed	RO 1st Pass Conc
pH	8.2	8.1
Langelier Saturation Index	0.91	1.37
Stiff & Davis Stability Index	-0.05	0.34
TDS[a] (mg/l)	35,987	65,511
Ionic Strength (molal)	0.74	1.39
HCO_3^- (mg/L)	107.7	193.3
CO_2 (mg/l)	0.44	0.98
CO_3^{-2} (mg/L)	14.25	27.59
$CaSO_4$ (% saturation)	22.4	46.8
$BaSO_4$ (% saturation)	0.00	0.00
$SrSO_4$ (% saturation)	15.5	35.9
CaF_2 (% saturation)	17.2	87.1
SiO_2 (% saturation)	0.80	1.5
$Mg(OH)_2$ (% saturation)	0.66	0.80

Footnotes:

[a]Total Dissolved Solids includes ions, SiO_2 and $B(OH)_3$. It does not include NH_3 and CO_2

Appendix B – Theoretical Energy Consumption

Equipment	Power Rating (kW)	Utilisation Per Hour	Theoretical Energy Usage Per Hour (kWh)
UF Feed Pump	18.5	95%	17.58
CIP Pump	7.5	8%	0.60
Backwash Pump	9.5	3%	0.29
UF Compressor	5.5	20%	1.10
RO Low Feed	22	100%	22.00
High Pressure 1	120	99%	118.80
High Pressure 2	11	99%	10.89
RO Compressor	1.5	10%	0.15
Control	1	100%	1.00
Lights	4	50%	2.00
Aircon	11	100%	11.00
Discharge Pump Set	30	100%	30.00

Legend

	Utilities
	Pre Filtration
	Reverse Osmosis
	Discharge Pumps

Appendix C – Municipal Invoices

ELECTRICITY INVOICE FOR THE PERIOD 17-12-2021 to 18-12-2021

ACTIVE ENERGY CHARGE

WINTER (June, July, August)	Peak	0.00	KWh	x		c/KWh	=
	Standard	0.00	KWh	x		c/KWh	=
	Off-Peak	0.00	KWh	x		c/KWh	=
SUMMER	Peak	485.60	KWh	x		c/KWh	=
	Standard	527.35	KWh	x		c/KWh	=
	Off-Peak	429.84	KWh	x		c/KWh	=
	Total kWhrs	1 442.79			Rand value for kWhr usage		

MAXIMUM DEMAND CHARGE

WINTER		0.00	KVA	x		R/KVA	=
SUMMER		171.20	KVA	x		R/KVA	=

					Active Energy & kVA charge Sub Total	=	
	per kWhr						
Voltage Surcharge		R 0.00		x	12 %	=	
Meter Number :					Basic Monthly Charge	=	
Meter Start Reading =		504 089.62			Sub Total excluding VAT	=	
Start Reading Date =		*17-12-2021*					
Meter End Reading =		505 532.41		VAT	15 %	=	
End Reading Date =		*18-12-2021*					
Consumption =		1 442.79			Total for Period	=	**R 0.00**

Maximum Demand 171.20 KVA on 17-12-2021 at 17:30

ELECTRICITY INVOICE FOR THE PERIOD 19-12-2021 to 18-01-2022

ACTIVE ENERGY CHARGE

WINTER (June, July, August)	Peak	0.00	KWh	x		c/KWh	=
	Standard	0.00	KWh	x		c/KWh	=
	Off-Peak	0.00	KWh	x		c/KWh	=
SUMMER	Peak	8 523.77	KWh	x		c/KWh	=
	Standard	18 603.19	KWh	x		c/KWh	=
	Off-Peak	37 456.95	KWh	x		c/KWh	=
	Total kWhrs	64 583.91			Rand value for kWhr usage		

MAXIMUM DEMAND CHARGE

WINTER		0.00	KVA	x		R/KVA	=
SUMMER		204.10	KVA	x		R/KVA	=

					Active Energy & kVA charge Sub Total		=
	per kWhr						
Voltage Surcharge				x	12 %		=
Meter Number :					Basic Monthly Charge		=
	Meter Start Reading =	505 532.41			Sub Total excluding VAT		=
	Start Reading Date =	*19-12-2021*					
	Meter End Reading =	570 116.32		VAT	15 %		=
	End Reading Date =	*18-01-2022*					
	Consumption =	64 583.91			Total for Period		=

Maximum Demand 204.10 KVA on 13-01-2022 at 23:00

ELECTRICITY INVOICE FOR THE PERIOD 19-01-2022 to 18-02-2022

ACTIVE ENERGY CHARGE

WINTER (June, July, August)	Peak	0.00	KWh	x		c/KWh	=
	Standard	0.00	KWh	x		c/KWh	=
	Off-Peak	0.00	KWh	x		c/KWh	=
SUMMER	Peak	17 519.93	KWh	x		c/KWh	=
	Standard	34 200.06	KWh	x		c/KWh	=
	Off-Peak	57 333.64	KWh	x		c/KWh	=
	Total kWhrs	109 053.63			Rand value for kWhr usage		

MAXIMUM DEMAND CHARGE

WINTER		0.00	KVA	x		R/KVA	=
SUMMER		207.30	KVA	x		R/KVA	=

					Active Energy & kVA charge Sub Total		=
	per kWhr						
Voltage Surcharge				x	12 %		=
Meter Number :					Basic Monthly Charge		=
Meter Start Reading =		570 116.32			Sub Total excluding VAT		=
Start Reading Date =		*19-01-2022*					
Meter End Reading =		679 169.95		VAT	15 %		=
End Reading Date =		*18-02-2022*					
Consumption =		109 053.63			Total for Period		=

Maximum Demand 207.30 KVA on 03-02-2022 at 19:00

ELECTRICITY INVOICE FOR THE PERIOD 19-02-2022 to 18-03-2022

ACTIVE ENERGY CHARGE							
WINTER (June, July, August)	Peak	0.00	KWh	x		c/KWh	=
	Standard	0.00	KWh	x		c/KWh	=
	Off-Peak	0.00	KWh	x		c/KWh	=
SUMMER	Peak	15 626.59	KWh	x		c/KWh	=
	Standard	32 612.81	KWh	x		c/KWh	=
	Off-Peak	57 984.78	KWh	x		c/KWh	=
	Total kWhrs	106 224.17			Rand value for kWhr usage		
MAXIMUM DEMAND CHARGE							
WINTER		0.00	KVA	x		R/KVA	=
SUMMER		222.50	KVA	x		R/KVA	=

			Active Energy & kVA charge Sub Total		=
Voltage Surcharge			x	12 %	=
Meter Number :				Basic Monthly Charge	=
Meter Start Reading =	679 169.95			Sub Total excluding VAT	=
Start Reading Date =	*19-02-2022*				
Meter End Reading =	785 394.12		VAT	15 %	=
End Reading Date =	*18-03-2022*				
Consumption =	106 224.17			Total for Period	=

Maximum Demand 222.50 KVA on 08-03-2022 at 18:30

Appendix D – Raw Data

Date	Production (m^3)	Date	Production (m^3)	Date	Production (m^3)
31-12-2021	558.00	**01-02-2022**	1104.00	**05-03-2022**	1082.00
01-01-2022	567.00	**02-02-2022**	1106.00	**06-03-2022**	1061.00
02-01-2022	559.00	**03-02-2022**	611.00	**07-03-2022**	859.00
03-01-2022	21.00	**04-02-2022**	282.00	**08-03-2022**	666.00
04-01-2022	0.00	**05-02-2022**	657.00	**09-03-2022**	676.00
05-01-2022	84.00	**06-02-2022**	886.00	**10-03-2022**	748.00
06-01-2022	574.00	**07-02-2022**	1100.00	**11-03-2022**	957.00
07-01-2022	702.00	**08-02-2022**	1079.00	**12-03-2022**	910.00
08-01-2022	239.00	**09-02-2022**	1120.00	**13-03-2022**	968.00
09-01-2022	956.00	**10-02-2022**	1086.00	**14-03-2022**	1117.00
10-01-2022	970.00	**11-02-2022**	1106.00	**15-03-2022**	1094.00
11-01-2022	963.00	**12-02-2022**	1102.00	**16-03-2022**	1055.00
12-01-2022	1008.00	**13-02-2022**	996.00	**17-03-2022**	371.00
13-01-2022	858.00	**14-02-2022**	979.00	**18-03-2022**	0.00
14-01-2022	942.00	**15-02-2022**	1038.00	**19-03-2022**	0.00
15-01-2022	773.00	**16-02-2022**	1074.00	**20-03-2022**	390.00
16-01-2022	789.00	**17-02-2022**	1055.00	**21-03-2022**	1057.00
17-01-2022	229.00	**18-02-2022**	1000.00	**22-03-2022**	950.00
18-01-2022	0.00	**19-02-2022**	1095.00	**23-03-2022**	780.00
19-01-2022	180.00	**20-02-2022**	1041.00	**24-03-2022**	649.00
20-01-2022	866.00	**21-02-2022**	760.00	**25-03-2022**	705.00
21-01-2022	861.00	**22-02-2022**	1051.00	**26-03-2022**	1050.00
22-01-2022	680.00	**23-02-2022**	985.00	**27-03-2022**	1005.00
23-01-2022	1038.00	**24-02-2022**	1102.00	**28-03-2022**	775.00
24-01-2022	993.00	**25-02-2022**	1067.00	**29-03-2022**	746.00
25-01-2022	1116.00	**26-02-2022**	848.00	**30-03-2022**	854.00
26-01-2022	739.00	**27-02-2022**	763.00	**31-03-2022**	793.00
27-01-2022	1091.00	**28-02-2022**	1047.00	**01-04-2022**	873.00
28-01-2022	1089.00	**01-03-2022**	1117.00	**02-04-2022**	879.00
29-01-2022	497.00	**02-03-2022**	1019.00	**03-04-2022**	911.00
30-01-2022	976.00	**03-03-2022**	1116.00		
31-01-2022	1082.00	**04-03-2022**	1097.00		

Appendix E – Inverter Datasheet

SUN2000-50KTL-M0

Smart String Inverter

Smart

Smart I-V Curve Diagnosis supported

Efficient

Max. efficiency 98.7%

Safe

Fuse free design

Reliable

Type II surge arresters for DC & AC

Efficiency Curve

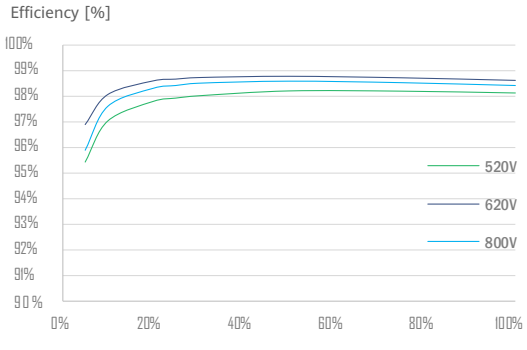

Circuit Diagram

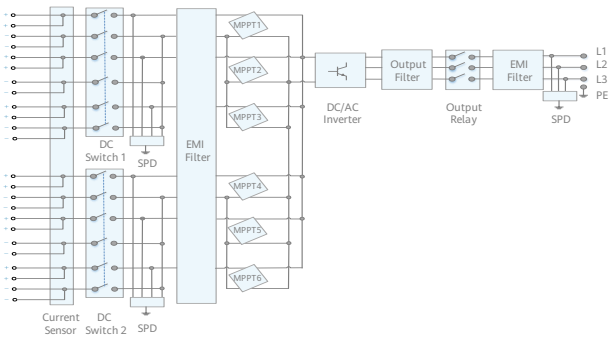

SUN2000-50KTL-M0

Technical Specification

Technical Specification	SUN2000-50KTL-M0
Efficiency	
Max. Efficiency	98.7%
European Efficiency	98.5%
Input	
Max. Input Voltage	1,100 V
Max. Current per MPPT	22 A
Max. Short Circuit Current per MPPT	30 A
Start Voltage	200 V
MPPT Operating Voltage Range	200 V ~ 1,000 V
Rated Input Voltage	600 V
Number of Inputs	12
Number of MPP Trackers	6
Output	
Rated AC Active Power	50,000 W
Max. AC Apparent Power	55,000 VA
Max. AC Active Power (cosϕ=1)	55,000 W
Rated Output Voltage	220 V / 380 V, 230 V / 400 V, default 3W + N + PE; 3W + PE optional in settings
Rated AC Grid Frequency	50 Hz / 60 Hz
Rated Output Current	76 A @380 V / 72.2 A @400 V
Max. Output Current	83.6 A @380 V / 79.4 A @400 V
Adjustable Power Factor Range	0.8 LG ... 0.8 LD
Max. Total Harmonic Distortion	<3%
Protection	
Input-side Disconnection Device	Yes
Anti-islanding Protection	Yes
AC Overcurrent Protection	Yes
DC Reverse-polarity Protection	Yes
PV-array String Fault Monitoring	Yes
DC Surge Arrester	Type II
AC Surge Arrester	Type II
DC Insulation Resistance Detection	Yes
Residual Current Monitoring Unit	Yes
Communication	
Display	LED Indicators, Bluetooth + APP
RS485	Yes
USB	Yes
Monitoring BUS (MBUS)	Yes
General Data	
Dimensions (W x H x D)	1,075 x 555 x 300 mm (42.3 x 21.9 x 11.8 inch)
Weight (with mounting plate)	74 kg (163.1 lb.)
Operating Temperature Range	-25°C ~ 60°C (-13°F ~ 140°F)
Cooling Method	Natural Convection
Max. Operating Altitude	4,000 m (13,123 ft.)
Relative Humidity	0 ~ 100%
DC Connector	Amphenol Helios H4
AC Connector	Waterproof PG Terminal + OT Connector
Protection Degree	IP65
Topology	Transformerless
Standard Compliance (more available upon request)	
Certificate	EN 62109-1/-2, IEC 62109-1/-2, EN 50530, IEC 62116, IEC 62910, IEC 60068, IEC 61683, IRR-DCC-MV, G99
Grid Code	IEC 61727, G59/3, DEWA, NRS 097-2-1, IEEE 1547, SASO, DEWA